Large-scale structure with gravitational waves. II. Shear

Fabian Schmidt and Donghui Jeong

Phys. Rev. D **86**, 083513 — Published 8 October 2012

DOI: 10.1103/PhysRevD.86.083513

Large-Scale Structure with Gravitational Waves II: Shear

Fabian Schmidt[1] and Donghui Jeong[2]

[1] *Theoretical Astrophysics, California Institute of Technology, Mail Code 350-17, Pasadena, CA 91125, USA*
[2] *Department of Physics and Astronomy, Johns Hopkins University, 3400 N. Charles St., Baltimore, MD 21210, USA*

The B- (curl-)mode of the correlation of galaxy ellipticities (shear) can be used to detect a stochastic gravitational wave background, such as that predicted by inflation. In this paper, we derive the tensor mode contributions to shear from both gravitational lensing and intrinsic alignments, using the gauge-invariant, full-sky results of Schmidt and Jeong [1]. We find that the intrinsic alignment contribution, calculated using the linear alignment model, is larger than the lensing contribution by an order of magnitude or more, if the alignment strength for tensor modes is of the same order as for scalar modes. This contribution also extends to higher multipoles. These results make the prospects for probing tensor modes using galaxy surveys less pessimistic than previously thought, though still very challenging.

PACS numbers: 98.65.Dx, 98.65.-r, 98.80.Jk

I. INTRODUCTION

A stochastic gravitational wave (GW) background is one of the key testable predictions of inflation. Thus, much theoretical and experimental effort is devoted to searching for this gravitational wave background. One necessary ingredient of any method designed to search for a GW background is the ability to cleanly separate the GW contribution from scalar perturbations. Most commonly, this is done by considering spin-2 quantities on the sky, such as the anisotropy in the polarization of the cosmic microwave background (CMB) radiation [2, 3], the anisotropy of the 2-point correlation function [4–7], or the ellipticity of galaxy images [8]. The polarization of the cosmic microwave background is commonly considered as the most promising probe. However, the 21cm emission from the dark ages has recently been shown to in principle offer even more discovery potential [5, 9]. On the other hand, previous authors have concluded that weak lensing shear will most likely not be a competitive probe of primordial GW [8, 10, 11]. Nevertheless, given the scientific impact, it will be crucial to confirm a possible detection of a GW background in the CMB with independent methods, such as shear.

The goal of this paper, and its companion [7], is to systematically and rigorously derive the GW effects on large-scale structure observables. While we restrict ourselves to a linear treatment in the tensor perturbations, we strive to keep the results as general as possible otherwise.

This paper deals with shear, i.e. the correlations of galaxy ellipticities. The underlying assumption in interpreting shear correlations is that in the absence of perturbations, galaxy ellipticities are uncorrelated on large scales. However, in the relativistic context, this raises the question of the *frame of reference* in which galaxy ellipticities are actually uncorrelated. In Schmidt and Jeong [1], we have derived an expression for the shear based strictly on observable quantities ("standard rulers"). As shown there, that expression is equivalent to the statement that galaxies are isotropically oriented in their local inertial frame, described by the Fermi normal coordinates along a given galaxy's geodesic.

Consider a region of spatial extent R, much larger than the size of individual galaxies but smaller than the typical wavelength of the perturbations we aim to measure through shear. The center of mass of this region moves on a time-like geodesic. We can construct a coordinate system where the center of mass is at rest at the origin, and the time coordinate t_F corresponds to the proper time of this geodesic. In other words, the unit vector defining the time coordinate is equal to the tangent vector to this geodesic. The spatial coordinate lines are chosen to be space-like geodesics ("straight lines") orthogonal to this time direction, and whose unit vectors are parallel-transported along the observer's geodesic. These are the so-called Fermi normal coordinates (FNC) [12, 13]. It is straightforward to construct them perturbatively for a given metric and time-like geodesic (see App. A). The most important property of Fermi normal coordinates is that the metric is Minkowski at the spatial origin at all times t_F, with corrections away from the geodesic going as $x_F^i x_F^j/R_c^2$, where x_F^i denote the spatial Fermi coordinates and R_c is the typical curvature scale of the space-time ($R_c \sim H^{-1}$ for an unperturbed FRW space-time). Thus, the Fermi normal coordinates are the frame in which a local observer in a weak gravitational field would describe her experiments. Neglecting the corrections $\propto x_F^2$, there is no preferred direction in these coordinates along which galaxies could align, and they thus have to be oriented isotropically. The contribution to the shear from the transformation to the local Fermi coordinates was first introduced by Dodelson et al. [8], who showed that this term, which they call "metric shear", has a significant impact on the observational signatures of tensor modes. Furthermore, as shown in [1], this term is crucial to ensure that the expression for the observable shear does not receive contributions from constant and pure-gradient metric perturbations, as required by coordinate-invariance.

Here, we evaluate this expression for the shear in an FRW space-time with tensor modes, which yields the shear contribution by "projection effects" induced by a GW background. As discussed in [7, 14], the tensor contributions typically peak at the source location rather than at lower redshifts, and there is no enhancement of the contribution by transverse modes. Both of these facts lead to qualitative differences from the scalar case.

As discussed, the space-time in Fermi coordinates around a given galaxy is not perfectly flat however, and the corrections to the metric $\propto x_F^i x_F^j/R_c^2$ provide preferred directions along which galaxies can align. For non-relativistic motions (which generally applies to large-scale structure), the relevant contribution to the metric in the Fermi frame corresponds to a tidal field, which can align galaxies and thus contribute to the observed shear correlation. Here we derive the contribution to the tidal field by tensor perturbations, and for the first time calculate the intrinsic alignment contribution of tensor modes in the linear alignment model. This prescription has been shown to agree well with observations on large scales in the scalar case. Note that this approach is only applicable for gravitational waves with periods much longer than the dynamical time of galaxies.

The key advantage of the shear applies to both lensing and linear intrinsic alignment contributions: linear scalar perturbations contribute only to the parity-even E-(gradient-)mode component at linear order, while tensor perturbations also contribute to the B-(curl-)mode (both through lensing and intrinsic alignments). Importantly, scalar perturbations do contribute to B-modes at second and higher order, a point which we will discuss in detail in § VI A.

The outline of the paper is a follows: we introduce our notation and conventions in § II (they are the same as in the companion paper [7]). § III presents the derivation of the lensing (projection) contribution, while § IV discusses the intrinsic alignment contribution from tensor modes. § V gives the expressions for the $E-$ and B-mode power spectrum of the shear, including the connection to previous results. § VI presents the results. We conclude in § VII. The appendix contains details on Fermi normal coordinates, the derivation of angular power spectra, and the connection to convergence and rotation.

II. PRELIMINARIES

We begin by introducing our convention for the metric and tensor perturbations and some notation; it is identical to that used in [7]. For simplicity, we restrict ourselves to a spatially flat FRW background, and consider only tensor (gravitational wave) modes in the main part of the paper. The perturbed metric is given by

$$ds^2 = a^2(\eta)\left[-d\eta^2 + (\delta_{ij} + h_{ij})\, dx^i dx^j\right], \qquad (1)$$

where h_{ij} is a metric perturbation which is assumed to be transverse and traceless:

$$h^i_{\ i} = 0 = (h_{ik})^{,i}. \qquad (2)$$

We then decompose h_{ij} into Fourier modes of two polarization states,

$$h_{ij}(\mathbf{k},\eta) = e^+_{ij}(\hat{\mathbf{k}})h^+(\mathbf{k},\eta) + e^\times_{ij}(\hat{\mathbf{k}})h^\times(\mathbf{k},\eta), \qquad (3)$$

where $e^s_{ij}(\hat{\mathbf{k}})$, $s = +,\times$, are transverse (with respect to $\hat{\mathbf{k}}$) and traceless polarization tensors normalized through $e^s_{ij}e^{s'\,ij} = 2\delta^{ss'}$. Note that $h_s = e^{ij}_s h_{ij}/2$. We assume both polarizations to be independent and to have equal power spectra:

$$\langle h_s(\mathbf{k},\eta)h_{s'}(\mathbf{k}',\eta')\rangle = (2\pi)^3\delta_D(\mathbf{k}-\mathbf{k}')\delta_{ss'}\frac{1}{4}P_T(k,\eta,\eta'). \qquad (4)$$

Here, η denotes conformal time, and the unequal-time power spectrum is given by

$$P_T(k,\eta,\eta') = T_T(k,\eta)T_T(k,\eta')P_{T0}(k), \qquad (5)$$

where $T_T(k,\eta)$ is the tensor transfer function, and the primordial tensor power spectrum is specified through an amplitude Δ^2_T and an index n_T via

$$P_{T0}(k) = 2\pi^2\, k^{-3}\left(\frac{k}{k_0}\right)^{n_T}\Delta^2_T. \qquad (6)$$

Following *WMAP* convention [15], we choose $k_0 = 0.002\,\mathrm{Mpc}^{-1}$ as pivot scale. Throughout, we will assume a scalar-to-tensor ratio of $r = 0.2$ at k_0 (consistent with the 95% confidence level WMAP bound), which together with our fiducial cosmology determines Δ^2_T. The tensor index is chosen to follow the inflationary consistency relation, $n_T = -r/8 = -0.0025$. For the expansion history, we assume a flat ΛCDM cosmology with $h = 0.72$ and $\Omega_m = 0.28$. Contributions from scalar perturbations are evaluated using a spectral index of $n_s = 0.958$ and power spectrum normalization at $z = 0$ of $\sigma_8 = 0.8$.

From Eq. (3) and Eq. (4), we easily obtain

$$\begin{aligned}\langle h_{ij}(\mathbf{k},\eta)h_{kl}(\mathbf{k}',\eta')\rangle &= (2\pi)^3\delta_D(\mathbf{k}-\mathbf{k}') \qquad (7)\\ &\quad\times\left[e^+_{ij}(\hat{\mathbf{k}})e^+_{kl}(\hat{\mathbf{k}}) + e^\times_{ij}(\hat{\mathbf{k}})e^\times_{kl}(\hat{\mathbf{k}})\right]\\ &\quad\times\frac{1}{4}P_T(k,\eta,\eta')\\ \langle h_{ij}(\mathbf{k},\eta)h^{ij}(\mathbf{k}',\eta')\rangle &= (2\pi)^3\delta_D(\mathbf{k}-\mathbf{k}')P_T(k,\eta,\eta').\end{aligned}$$

Long after recombination, the transverse anisotropic stress which sources gravitational waves becomes negligible, and the tensor modes propagate as free waves. During matter-domination, the tensor transfer function then simply becomes

$$T_T(k,\eta) = 3\frac{j_1(k\eta)}{k\eta}, \qquad (8)$$

which however is still valid to a high degree of accuracy during the current epoch of acceleration. We will use Eq. (8) throughout. We also define

$$\mathcal{P}^{ij} = \delta^{ij} - \hat{n}^i \hat{n}^j \tag{9}$$

as the projection operator perpendicular to the line of sight.

As a traceless 2-tensor on the sphere, the shear can be decomposed into spin±2 functions ${}_{\pm 2}\gamma = \gamma_1 \pm i\gamma_2$ (in analogy to the combination of Stokes parameters $Q \pm iU$ for radiation) as

$$\gamma_{ij} = {}_2\gamma\, m^i_+ m^j_+ + {}_{-2}\gamma\, m^i_- m^j_-. \tag{10}$$

Here, we have defined the unit vectors of the circularly polarized basis, $\mathbf{m}_\pm \equiv (\mathbf{e}_\theta \mp i\,\mathbf{e}_\phi)/\sqrt{2}$ (see App. A in [1]). If we choose a coordinate system where $\hat{n}^i$ is along the z-axis and e^i_θ along the x-axis, we have

$$\gamma_{ij} = \begin{pmatrix} \gamma_1 & \gamma_2 & 0 \\ \gamma_2 & -\gamma_1 & 0 \\ 0 & 0 & 0 \end{pmatrix}. \tag{11}$$

This decomposition is particularly useful for deriving multipole coefficients and angular power spectra. In particular, we can define the multipole moments of the parity-even E-modes and parity-odd B-modes through

$$\begin{aligned} a^{\gamma E}_{lm} &= \frac{1}{2}\left(a^\gamma_{lm} + a^{\gamma *}_{lm}\right) \\ a^{\gamma B}_{lm} &= \frac{1}{2i}\left(a^\gamma_{lm} - a^{\gamma *}_{lm}\right). \end{aligned} \tag{12}$$

We also define

$$\begin{aligned} X_\pm &\equiv m^i_\mp X_i \\ E_\pm &\equiv m^i_\mp m^j_\mp E_{ij} \end{aligned} \tag{13}$$

for any vector X_i and tensor E_{ij}.

III. LENSING EFFECTS

We begin with the definition of shear in the relativistic context as derived in [1], for a synchronous comoving metric as in Eq. (1):

$$\begin{aligned} {}_{\pm 2}\gamma &\equiv m^i_\mp m^j_\mp \mathcal{A}_{ij} \\ &= -\frac{1}{2} h_\pm - m^i_\mp m^j_\mp \partial_{\perp\, i} \Delta x_{\perp\, j}. \end{aligned} \tag{14}$$

In other words, the shear is the traceless part of the symmetric 2×2 matrix $\mathcal{A}_{ij}$ which describes the transverse distortion of transverse standard rulers. $\Delta x^i_\perp$ is the displacement perpendicular to the line of sight of the observed position from the true position of the source, in terms of the global comoving coordinates.

As shown in [1], Eq. (14) is explicitly given by

$$\begin{aligned} ({}_{\pm 2}\gamma)(\hat{\mathbf{n}}) = &-\frac{1}{2} h_{\pm\, o} - \frac{1}{2} h_\pm \\ &- \int_0^{\tilde{\chi}} d\chi \Bigg\{ \frac{\tilde{\chi} - \chi}{2} \frac{\chi}{\tilde{\chi}} (m^i_\mp m^j_\mp \partial_i \partial_j h_{kl}) \hat{n}^k \hat{n}^l \\ &+ \left(1 - 2\frac{\chi}{\tilde{\chi}}\right) \hat{n}^l m^k_\mp m^i_\mp \partial_i h_{kl} - \frac{1}{\tilde{\chi}} h_\pm \Bigg\}. \end{aligned} \tag{15}$$

The last term in the first line of this equation can be understood as coming from the transformation from global coordinates to the local Fermi normal coordinates [1]; in the following we will refer to this as the "FNC term". It is immediately clear that a constant metric perturbation h_{ij} (which corresponds to a pure gauge mode) does not contribute to $\gamma_1 \pm i\gamma_2$. The same is true for a pure gradient $h_{ij} = B_{ijk} x^k$. In App. C of [1] we have applied several test cases to Eq. (15), including a Bianch I cosmology where all terms contribute non-trivially.

IV. INTRINSIC EFFECTS

Eq. (15) is derived assuming we have a perfect standard ruler, in the sense that the intrinsic physical size of the ruler is uncorrelated with the perturbations h_{ij}. In the case of weak lensing shear surveys, the "standard ruler" is the fact that galaxies are randomly oriented, i.e. their apparent size measured along two different fixed directions is on average equal. However, we know that in reality galaxy orientations are not truly random, but there is some alignment with large-scale tidal fields.

In order to determine the effective tidal field experienced by galaxies in a Universe with propagating tensor modes, we derive the corrections $\propto x_F^2$ to the metric $g^F_{\mu\nu}$ in the Fermi normal coordinate frame. In particular, since we are concerned with non-relativistic motions, we are mostly interested in the time-time part of the metric g^F_{00}. The detailed derivation for a space-time described by Eq. (1) is presented in App. A. The result for g^F_{00} is

$$g^F_{00}(\mathbf{x}_F, t_F) = -1 + (\dot{H} + H^2) r_F^2 - 2\Psi^F(\mathbf{x}_F, t_F) \tag{16}$$

$$\Psi^F(\mathbf{x}_F, t_F) = -\frac{1}{4}[\ddot{h}_{ij}(\mathbf{0}, t_F) + 2H(t_F)\dot{h}_{ij}(\mathbf{0}, t_F)] x^i_F x^j_F, \tag{17}$$

where $r_F^2 = \delta_{ij} x^i_F x^k_F$, and dots indicate derivatives with respect to time t (equivalent to t_F at this order). The terms $\propto r_F^2$ in Eq. (16) are the usual Hubble drag which provide an effective repulsive force. The leading effect of large-scale cosmological perturbations on the region considered is to add an effective tidal field Ψ^F, which depends on the time derivatives of the metric perturbation h_{ij}. Note that for a traceless tensor perturbation, Ψ^F is indeed a purely tidal field (i.e. $\nabla^2 \Psi^F = 0$). The fact that the amplitude of the tidal field is given by the time derivatives of the tensor modes implies that only modes that

have entered the horizon contribute; through Eq. (8), the terms are seen to be of order k/H and $(k/H)^2$.

In the absence of perturbations ($h_{ij} = 0$), Eq. (16) is isotropic. Thus, in the Fermi frame, there is no preferred direction along which galaxies forming in this region could align, and their orientations are truly random in this case. As shown in [1], the expression for the shear Eq. (14) contains precisely this statement (of course this holds not only for galaxy orientations, but any standard ruler).

In the presence of perturbations, the tidal field $\propto x^i_F x^j_F$ provides a preferred direction along which galaxies can align. The fact that large-scale tidal fields tend to align galaxies (intrinsic alignment, IA) is well established both theoretically and observationally for scalar perturbations (e.g., [16–18]). In order to make progress, we will adopt the linear alignment (LA) model, which has recently been shown to be consistent with observations on large scales ($\gtrsim 10\,\mathrm{Mpc}/h$) [19, 20]. In this model (following the notation of [19]), the tidal tensor t_{ij} at the location of the galaxy, defined through

$$t_{ij} = \left(\partial_i\partial_j - \frac{1}{3}\delta_{ij}\nabla^2\right)\Psi, \tag{18}$$

contributes to the traceless part of the observed distortion matrix $\mathcal{A}_{ij}$ of the galaxy image through

$$\begin{aligned}\mathcal{A}^{\rm IA}_{ij}(\hat{\mathbf{n}}) =& -\frac{C_1}{4\pi G}\mathcal{P}_{ik}\mathcal{P}_{jl}t^{kl}(z_p)\\ =& -\frac{2}{3}C_1\rho_{\rm cr0}H_0^{-2}\mathcal{P}_{ik}\mathcal{P}_{jl}\,t^{kl}(z_p).\end{aligned} \tag{19}$$

That is, $\mathcal{A}^{\rm IA}_{ij}$ is proportional to the projection of the tidal tensor onto the sky plane. Here, $\rho_{\rm cr0} = 3H_0^2/(8\pi G)$ is the critical density today. The constant of proportionality C_1 determines the magnitude of alignment, while z_p, the redshift at which the tidal field is evaluated, is another parameter of the model. Observationally, $C_1\rho_{\rm cr0} \sim 0.1$ for galaxies at redshifts less than 1, when choosing z_p to be equal to the source redshift. A positive C_1, together with the overall sign in Eq. (19), corresponds to a galaxy's major axis aligning with the *smallest* eigenvector of t_{ij}; physically, an initially spherical perturbation will tend to collapse last in the direction of the smallest potential curvature, leading to a preferential alignment of the major axis with this direction. Note that in Eq. (19), $C_1\rho_{\rm cr0}$ multiplies the tidal field in physical rather than comoving units.

While this mechanism is expected to be qualitatively the same for tensor modes as for scalar modes, there is no reason for the amplitude C_1 to be the same in both cases. In particular, linear tidal fields sourced by scalar perturbations are constant during matter domination, while tensor perturbations decay and oscillate. However, we will see that the tensor modes relevant for the IA contribution are long-wavelength and should not have a qualitatively different impact on the formation of galaxies than scalar tidal fields. We will return to this issue in § VI. In the following, we will assume that z_p is equal to the source redshift. Generally, evaluating the tidal field at $z_p > \tilde{z}$ leads to larger effects so that this is a conservative assumption.

Using Eq. (17) and Eq. (14), it is then straightforward to evaluate the contribution of tensor modes to the shear ${}_{\pm2}\gamma$:

$$\begin{aligned}({}_{\pm2}\gamma)^{\rm IA}(\hat{\mathbf{n}}) &= m^i_{\mp}m^j_{\mp}\mathcal{A}^{\rm IA}_{ij}\\ &= \frac{1}{3}C_1\rho_{\rm cr0}H_0^{-2}\left(\ddot{h}_{\pm} + 2H\dot{h}_{\pm}\right)\\ &= \frac{1}{3}C_1\rho_{\rm cr0}H_0^{-2}a^{-2}\left(h''_{\pm} + aHh'_{\pm}\right),\end{aligned} \tag{20}$$

where primes indicate derivatives with respect to η, and we have used $dt = ad\eta$.

V. OBSERVED SHEAR STATISTICS

We now use the results derived in the previous two sections to calculate the angular power spectrum of the observed shear induced by tensor modes. We briefly outline the steps of the derivation, which follows the general prescription described in App. A1 of [1], with details relegated to App. B.

In the first step, we consider a single tensor mode of wavevector $\mathbf{k}$ which we assume oriented along the z-axis. Including the intrinsic alignment contribution (§ IV), we obtain for the contribution to the shear

$$\begin{aligned}({}_{\pm2}\gamma)(\mathbf{k},\hat{\mathbf{n}}) = \sum_{p=-1,1}\Bigg\{ &-\frac{1}{2}\left[h_p(\mathbf{k},\eta_0) + \left(1 - \frac{2}{3}C_1\rho_{\rm cr0}H_0^{-2}\tilde{a}^{-2}\left\{\partial^2_{\tilde{\eta}} + \tilde{a}\tilde{H}\partial_{\tilde{\eta}}\right\}\right)h_p(\mathbf{k},\tilde{\eta})e^{i\mathbf{k}\cdot\hat{\mathbf{n}}\,\tilde{\chi}}\right]\frac{1}{2}(1\mp p\mu)^2 e^{i2p\phi}\\ &+\int_0^{\tilde{\chi}} d\chi\left[\frac{\tilde{\chi}-\chi}{4}\frac{\chi}{\tilde{\chi}}k^2(1-\mu^2)^2 + \left(1-2\frac{\chi}{\tilde{\chi}}\right)i\frac{k}{2}(1-\mu^2)(1\mp p\mu) + \frac{1}{2\tilde{\chi}}(1\mp p\mu)^2\right]\\ &\times e^{i2p\phi}h_p(\mathbf{k},\eta_0-\chi)e^{i\mathbf{k}\cdot\hat{\mathbf{n}}\,\chi}\Bigg\},\end{aligned}$$

where $h_{\pm1} = (h_+ \mp i h_\times)/2$ are the circular polarization states of tensor modes, $\mu = \cos\theta$, and θ, ϕ denote the polar and azimuthal angles of the line of sight unit vector $\hat{\mathbf{n}}$. We then apply the spin-lowering/raising operator twice to ${}_{\pm2}\gamma$ in order to obtain a rotationally invariant (spin-0) quantity. The spherical harmonic coefficients of this scalar quantity are directly related to those of the spin$\pm$2 shear components (see App. A in [1]). We can then separate a^γ_{lm} into a real part $a^{\gamma E}_{lm}$, which is parity-even and thus transforms in the same way as a tensor derived from a scalar function f, and an imaginary part $i\, a^{\gamma B}_{lm}$, which acquires an additional minus sign under parity. This E/B-mode decomposition is useful because any symmetric tensor γ_{ij} derived from a scalar function is parity-even and thus does not source any B-modes (as shown explicitly for the shear in [1]). Further, any perturbations generated by parity-conserving physics do no induce an $E-B$ cross-correlation.

Finally, using relations derived in App. A1 of [1], we obtain the angular power spectra of E- and B-modes of the shear induced by tensor modes (App. B 2):

$$
\begin{aligned}
C^{XX}_\gamma(l) &= \frac{1}{2\pi}\int k^2 dk\, P_{T0}(k) |F^{\gamma X}_l(k)|^2, \qquad X = E,\, B \qquad (21)\\
F^{\gamma E}_l(k) \equiv & -\frac{1}{4}\left[T_T(k,\eta_0)\left(\mathrm{Re}\,\hat{Q}_1(x)\frac{j_l(x)}{x^2}\right)_{x=0} + \left(1 - \frac{2}{3}C_1\rho_{\rm cr0}H_0^{-2}\tilde{a}^{-2}\left\{\partial^2_{\tilde\eta} + \tilde{a}\tilde{H}\partial_{\tilde\eta}\right\}\right) T_T(k,\tilde\eta)\mathrm{Re}\,\hat{Q}_1(\tilde{x})\frac{j_l(\tilde{x})}{\tilde{x}^2}\right]\\
& + \int_0^{\tilde\chi}\frac{d\chi}{\chi}\left[\mathrm{Re}\,\hat{Q}_2(x) + \frac{\chi}{\tilde\chi}\mathrm{Re}\,\hat{Q}_3(x)\right]\frac{j_l(x)}{x^2}T_T(k,\eta_0-\chi)\\
F^{\gamma B}_l(k) \equiv & -\frac{1}{4}\left[T_T(k,\eta_0)\left(\mathrm{Im}\,\hat{Q}_1(x)\frac{j_l(x)}{x^2}\right)_{x=0} + \left(1 - \frac{2}{3}C_1\rho_{\rm cr0}H_0^{-2}\tilde{a}^{-2}\left\{\partial^2_{\tilde\eta} + \tilde{a}\tilde{H}\partial_{\tilde\eta}\right\}\right) T_T(k,\tilde\eta)\mathrm{Im}\,\hat{Q}_1(\tilde{x})\frac{j_l(\tilde{x})}{\tilde{x}^2}\right]\\
& + \int_0^{\tilde\chi}\frac{d\chi}{\chi}\mathrm{Im}\,\hat{Q}_2(x)\frac{j_l(x)}{x^2}T_T(k,\eta_0-\chi).
\end{aligned}
$$

Here $\hat{Q}_i(x)$ are derivative operators whose action on $j_l(x)/x^2$ is given explicitly in Eq. (B16); in particular $\mathrm{Im}\,\hat{Q}_3(x)[j_l(x)/x^2] = 0$.

A. Relation to convergence and rotation

The shear is most commonly written in terms of angular derivatives of the deflection angle $\Delta\theta^i$, i.e. γ_{ij} is defined as the trace-free part of $\partial\Delta\theta_j/\partial\theta_i$. In our notation, $\Delta\theta^i = \Delta x^i_\perp/\tilde\chi$, and $\partial\Delta\theta_j/\partial\theta_i = \partial_{\perp i}\Delta x_{\perp j}$. There are two degrees of freedom in $\Delta x^i_\perp$, and hence only two independent components of $\partial_{\perp i}\Delta x_{\perp j}$. If we define the convergence $\hat\kappa$ and rotation ω through

$$
\begin{aligned}
\hat\kappa &\equiv -\frac{1}{2}\partial_{\perp i}\Delta x^i_\perp\\
\omega &\equiv -\frac{1}{2}\varepsilon_{ijk}\hat{n}^i\partial^j_\perp\Delta x^k_\perp, \qquad (22)
\end{aligned}
$$

then the E-mode of the shear defined as trace-free part of $\partial_{\perp i}\Delta x_{\perp j}$ is directly related to $\hat\kappa$, while the B-mode is related to ω. As shown by Stebbins [21], on the full sky

$$
\begin{aligned}
C^{EE}_\gamma(l) &= \frac{(l+2)(l-1)}{l(l+1)}C_{\hat\kappa}(l)\\
C^{BB}_\gamma(l) &= \frac{(l+2)(l-1)}{l(l+1)}C_\omega(l). \qquad (23)
\end{aligned}
$$

However, neither of the deflection angle $\Delta x^i_\perp$, the convergence $\hat\kappa$, or the shear defined as trace-free part of $\partial_{\perp i}\Delta x_{\perp j}$ are observable (the rotation is only observable if there is an intrinsic preferred direction in the source plane). Instead, the observable shear is given by Eq. (15) which includes the FNC term. Nevertheless, the relations Eq. (23) are useful as an analytical and numerical cross-check of Eq. (21) (without the IA contribution), and this cross-check is presented in App. C.

In the previous work of [8], the rotation was used as a proxy for shear B-modes through Eq. (23). This result thus does not include the FNC term. However, they also consider the "metric shear", which is the contribution to ω that corresponds to the shear contribution by the FNC term. When including the metric shear in ω, we indeed recover the B-modes of the shear including the FNC term through the relation Eq. (23) (see App. C 2). Thus, our results for the lensing-induced shear B-modes from tensor modes (i.e., neglecting the intrinsic alignment contribution) agree with those of [8], modulo the factor $(l+2)(l-1)\,/\,l(l+1)$.

VI. RESULTS

We begin by investigating the separate terms contributing to the shear E- and B-mode power spectra in Eq. (21), focusing on the lensing contributions without intrinsic alignment first. Fig. 1 shows the E-mode angular power spectra obtained by separately considering only the terms $\propto \hat{Q}_2$, $\propto \hat{Q}_3$, and the FNC and observer terms $\propto \hat{Q}_1$. Here, we have multiplied the power spectra by l^6 as they are very steeply falling with l. We see that for $l \lesssim 10$ there is a very significant cancellation (by

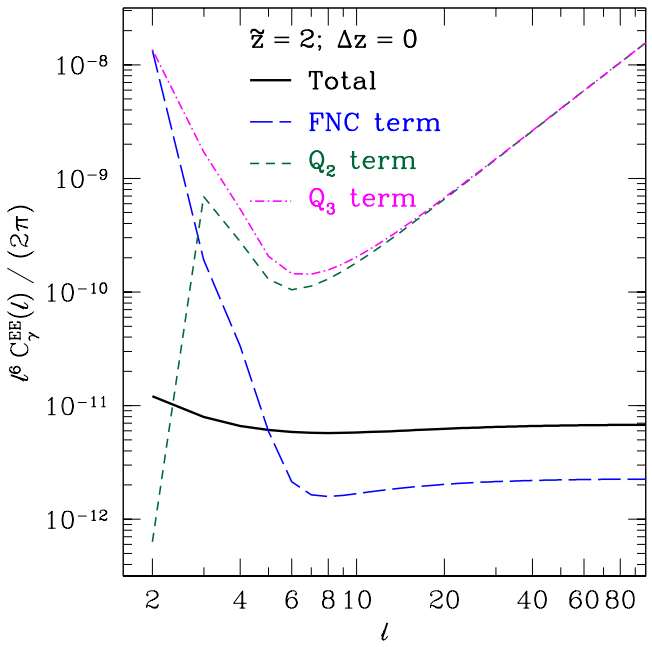

FIG. 1: Lensing (projection) contributions to the observed angular power spectrum of the E-mode component of the shear from tensor modes, separated into terms $\propto \hat{Q}_1$ (observer and FNC terms), $\propto \hat{Q}_2$ and $\propto \hat{Q}_3$ respectively. Note that power spectra are multiplied by l^6. We have assumed a sharp source redshift of $\tilde{z} = 2$.

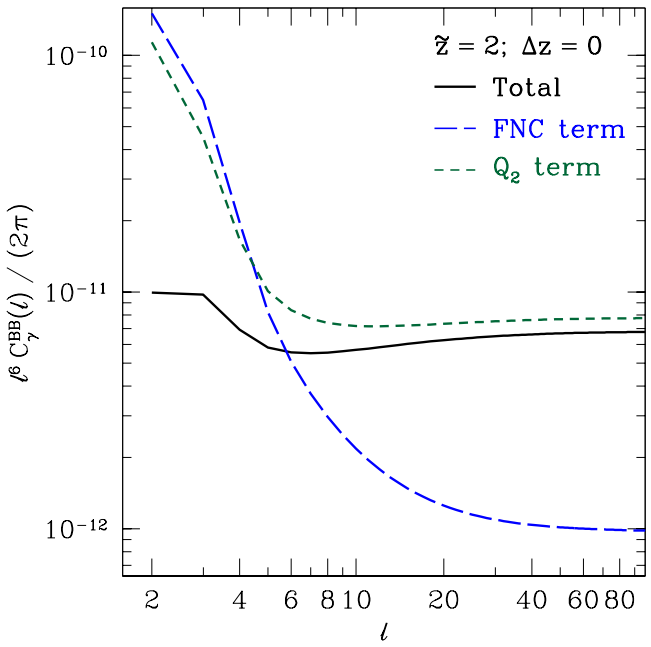

FIG. 2: Same as Fig. 2, but for the B-mode component.

three orders of magnitude) between the different terms. In fact, the magnitude of the individual terms depends on the lower limit used in the integration over k, and diverges logarithmically as $k_{\rm min} \to 0$ for small l. For the B-modes, the cancellation is not as important, though still significant (Fig. 2; in this case there is no $\hat{Q}_3$ term). This result is in agreement with the findings of [8]: when including the FNC contribution (metric shear), the amplitude decreases significantly. This is not surprising: if we drop the FNC term in Eq. (21), tensor perturbations with $k \to 0$ contribute to the shear at low l, and since the tensor power spectrum is sharply falling with k, these contributions are large. Clearly, these contributions are unphysical however, and the FNC term must be included.

Fig. 3 shows the total lensing contribution to the E-mode power spectrum of the shear, the intrinsic alignment contribution, as well as the sum of the two, while Fig. 4 shows the same for the (more interesting) B-modes. Here, we assumed a Gaussian redshift distribution $dN/d\tilde{z} \propto \exp(-(\tilde{z}-\bar{z})^2/2\Delta z^2)$ with $\Delta z = 0.03(1+\bar{z})$. Further, we have adopted a value of $C_1\rho_{\rm cr0} = 0.12$ as measured in the Sloan Digital Sky Survey [19]. This coefficient will depend on the specific galaxy sample considered, in particular on the redshift. Here we extrapolate the value of $C_1\rho_{\rm cr0}$ measured for galaxies at $z \approx 0.3-0.5$ to galaxies at $z = 2$, assuming no evolution. Thus our results should only be seen as a rough estimate of the magnitude of this effect (note however that we assume a constant alignment strength with respect to the physical, not comoving tidal field). Even with this caveat in mind however, it is clear that the intrinsic alignment contribution is far larger than the lensing contribution. This is in contrast to the scalar case, where for source galaxies at cosmological redshifts the lensing signal is significantly larger than the intrinsic alignment contribution. The underlying reason is that the projected contributions from lensing are relatively suppressed in the tensor case. While scalar perturbations with transverse wavevector deflect light coherently along the past line cone to the source, tensor perturbations propagate and decay, such that no such coherent deflection occurs even for transverse wavevectors [14]. The result is that the lensing contributions are mostly localized at the source for tensor modes, and down-weighted by the lensing kernel ($\propto \tilde{\chi} - \chi$).

Apart from $C_1\rho_{\rm cr0}$, the linear alignment model has another free parameter in the redshift z_p at which the tidal field is evaluated. By default, we choose $z_p = \tilde{z}$. However, choosing z_p to correspond to a time 5×10^8 years before observation ($z_p \approx \tilde{z} + 0.04$ for $\tilde{z} = 2$), which corresponds to several dynamical times for typical galaxies, only yields a slight increase in the power spectrum contribution by $\sim$3%. Varying z_p thus does not have a significant impact on the intrinsic alignment contribution. On the other hand, this mild dependence on z_p indicates that the bulk of the IA contribution induced by tensor modes is due to slowly varying tidal fields, i.e. tensor modes with $k/H \sim 1$, rather than rapidly oscillating modes with $k/H \gg 1$ (this is confirmed by numerical inspection of the intrinsic alignment contribution to

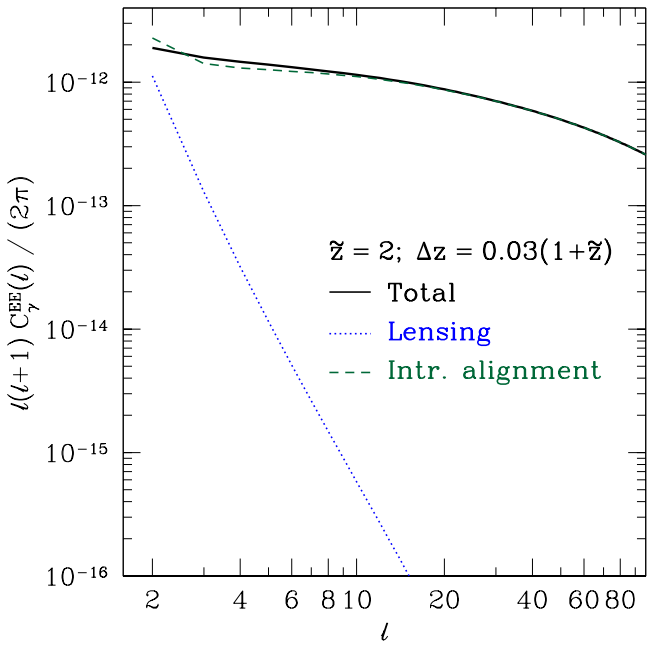

FIG. 3: Angular power spectrum of the observed E-component of the shear from lensing and intrinsic alignment affects, as well as the total power spectrum. We assumed $C_1\rho_{\rm cr0} = 0.12$ (following the results of [19]), and a Gaussian distribution of source redshifts centered at $\tilde{z} = 2$ with RMS width of $\Delta z = 0.03(1+\tilde{z})$.

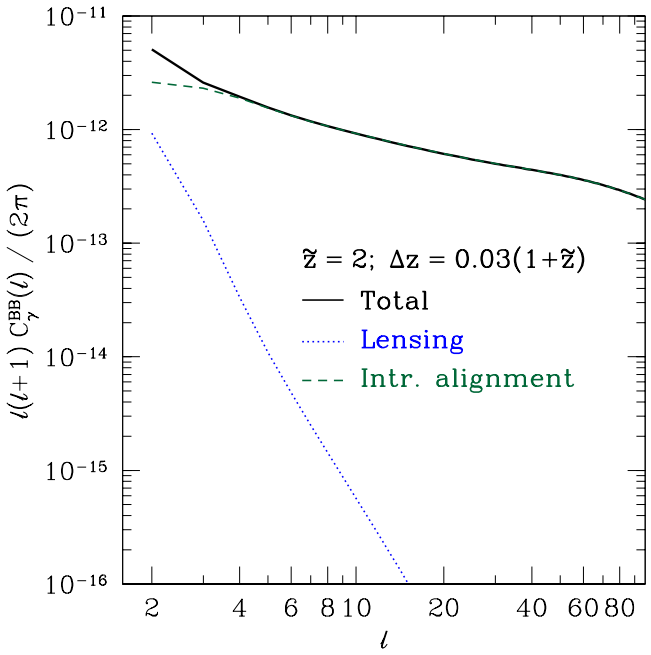

FIG. 4: Same as Fig. 3, but for B-modes.

$F_l^{E,B}$). Such tidal fields, which vary on a Hubble time, are not expected to have a qualitatively different effect on the formation of galaxies and halos than scalar tidal fields, given that the relevant time scale is the dynamical time of the collapsing dark matter halo. We thus expect that the value of $C_1\rho_{\rm cr0}$ relevant for the IA contributions to shear from tensor modes will not be very different from that for scalar tidal fields. However, one would expect $C_1\rho_{\rm cr0}$ to be generically scale-dependent for tensor modes, decaying from its low-k limit to smaller values as $1/k$ approaches the scale of halos and galaxies ($k \gtrsim 0.3\,h/{\rm Mpc}$).

Fig. 5 shows the redshift evolution of the B-modes of the shear. As expected, larger source redshifts yield significantly larger signals, due to the decay of the tensor modes and since at higher redshifts, larger scales are being probed at a given l. However, we also see that the intrinsic alignment contribution evolves even faster with source redshift (note that here we have assumed the same value for $C_1\rho_{\rm cr0}$ at all redshifts). This can be traced back to the factor of $\tilde{a}^{-2}$ in the IA contribution [Eq. (21)], which is due to the transformation from conformal time derivatives to physical time derivatives. It is also interesting to consider the dependence of the signal on the width of the source galaxy redshift distribution. This is illustrated in Fig. 6. The lensing contributions are largely independent of Δz for the range of multipoles relevant here. On the other hand, the IA contribution is noticeably increased for sharp source redshifts at $l \gtrsim 10$, a consequence of the fact that this contribution is not projected along the line of sight but evaluated at the source. Thus, unlike the lensing contribution, the IA contribution is essentially a three-dimensional field. Note also that in this case $l(l+1)C_\gamma^{BB}(l) \approx$ const, i.e. there is roughly equal power per decade in multipole for the IA contribution. However, following our discussion above, we expect the approximation of a scale-independent alignment coefficient to break down once the wavelength of contributing tensor modes approaches the scale of halos, roughly at l greater than a few hundred.

A. B-modes from scalar perturbations

In addition to being sourced by primordial tensor modes, shear B-modes are also produced by second-order corrections to lensing by scalar perturbations. These come from three sources.

The first source is tensor modes generated by nonlinear gravitational instability (e.g., [22, 23]). The shear B-mode power spectrum induced by these tensor modes was found to be roughly scale-invariant and at the level of $l(l+1)C^{BB}(l)/2\pi \approx 10^{-14}$ [10] which is much smaller than the total primordial GW signal presented here for $r = 0.2$. However, the calculation of [10] did not include the intrinsic alignment effect which will also increase the B-mode signal of scalar-induced tensor modes. Due to the different scale-dependence and redshift evolution of the latter, the boost will likely be somewhat smaller than

that for the primordial tensor modes. We leave this for future work.

The second, more significant scalar source for B-modes is from second-order corrections in the geodesic equation (beyond-Born correction and lens-lens coupling) [24, 25]. We have evaluated these according to

$$C_\gamma^{BB} = \frac{(l+2)(l-1)}{l(l+1)} C_l^{\omega\omega}, \tag{24}$$

where $C_l^{\omega\omega}$ is given in Eq. (51) of [24]. Note that the expression given there uses the Limber and flat-sky approximations and is thus not expected to be accurate for $l \lesssim 10$. We compare this contribution with the total contribution from primordial tensor modes (intrinsic alignment and lensing) in Fig. 7. At $z = 2$, the scalar contributions become larger than the tensor mode signal at $l \gtrsim 6$. For higher redshifts, they only dominate at higher l.

Finally, a third contribution comes from the fact that observationally we measure the reduced shear $g = \gamma/(1-\kappa)$ [26, 27]. Furthermore, selection effects ("lensing bias") lead to a similar second order correction [28]. At leading order, both contributions can be summarized by writing the observed shear tensor as

$$\gamma_{ij}^{\rm obs}(\hat{\mathbf{n}}) = \gamma_{ij}(\hat{\mathbf{n}}) + (1+q)\hat{\kappa}(\hat{\mathbf{n}})\gamma_{ij}(\hat{\mathbf{n}}), \tag{25}$$

where the parameter q parametrizes the lensing bias contribution [28]. We can evaluate the scalar B-mode contribution from both of these effects using Eq. (21) in [28]. Note that this equation was derived in the flat-sky limit and hence will also not be accurate at $l \lesssim 10$. This contribution is also shown in Fig. 7 (assuming a lensing bias coefficient of $q = 1$). This contribution is even larger than that from the second order Born correction, and in fact dominates over the primordial GW contribution at $\tilde{z} = 2$ for all l but $l = 2$. In principle one could reduce this contribution significantly by selecting a source galaxy sample with $q \approx -1$, although whether this is feasible in practice would need to be investigated. The fact that the reduced shear and lensing bias contributions produce the dominant scalar contribution to shear B-modes is an interesting result in itself and has not been pointed out before.

VII. DISCUSSION

In this paper, we have studied the shear induced by a primordial GW background. In addition to the projection (lensing) effects, for which we use a gauge-invariant expression, we derive for the first time the contribution due to intrinsic alignment (IA) of galaxies through the effective tidal field induced by tensor modes. We have found that this contribution is typically much larger than that from lensing. While surprising initially, this is due to the qualitatively different properties of lensing by tensor modes as compared to scalar modes.

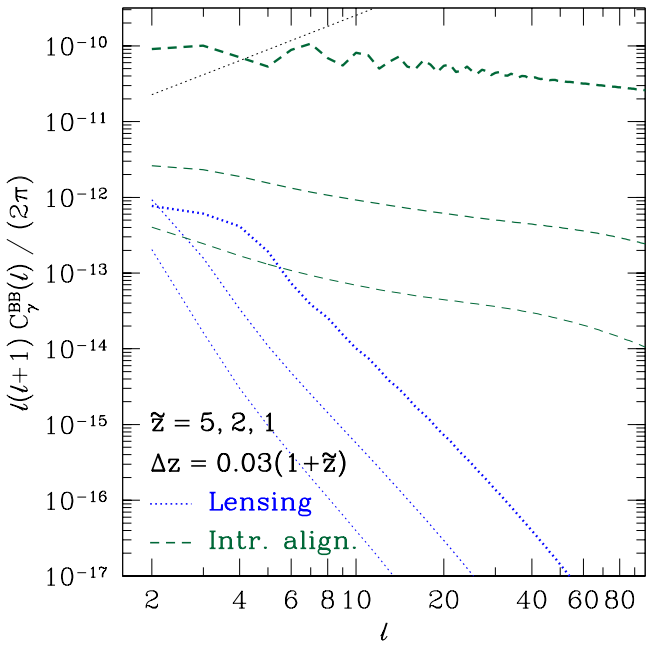

FIG. 5: Dependence of the lensing and intrinsic alignment contributions to the B-mode shear power spectrum on the source redshift $\tilde{z}$. We have assumed a Gaussian redshift distribution centered at $\tilde{z} = 5,\ 2,\ 1$ (from top to bottom), and RMS width $\Delta z = 0.03(1+\tilde{z})$. The black dotted line near the top of the figure shows the 1σ error on the shear power spectrum per multipole induced by shape noise [Eq. (27)], for a survey with $\bar{n} = 100\,\mathrm{arcmin}^{-2}$, $\sigma_e = 0.3$, and $f_{\rm sky} = 0.5$.

The IA contribution depends on a coefficient which can be observationally determined for scalar perturbations. In general, this does not have to be the same for tensor modes, since tensor modes evolve while the scalar tidal field is constant on large scales (during matter domination). On the other hand, the bulk of the tensor contributions is from horizon-scale modes, which evolve on the Hubble time scale. Compared to the dynamical time of galaxies and halos, this is a very slow evolution, and we expect the alignment coefficient to only be mildly affected by this. On the other hand, the results shown in Fig. 3 through 6 depend on the alignment strength at high redshifts, which is currently poorly known observationally.

The IA contribution also decays much more slowly towards high l than the lensing contribution (especially for narrow source redshift distributions). In principle, this could allow one to access smaller-scale tensor modes than those probed by the cosmic microwave background. Further, since the IA contribution is not projected along the light cone, this effect in principle allows us to measure the entire three-dimensional field of tensor perturbations. In the case of perfect redshift measurements, the number of tensor modes measurable up to a maximum scale would thus scale as $k_{\rm max}^3$ rather than $l_{\rm max}^2$.

On the other hand, even with this increased signal, the

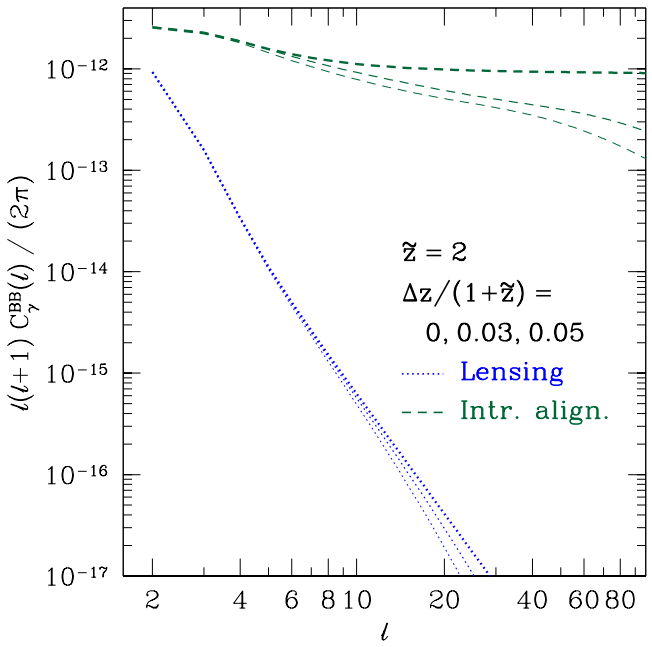

FIG. 6: Dependence of the lensing and intrinsic alignment contributions to the B-mode shear power spectrum on the width of the source redshift distribution Δz. $\tilde{z} = 2$ for all curves.

requirements for a detection of a stochastic GW background using galaxy ellipticities are still extremely challenging. Purely in terms of statistical power, the intrinsic ellipticities of galaxies add noise ("shape noise") to the shear E- and B-mode power spectra. The corresponding 1σ error on the power spectrum per multipole is given by

$$\Delta C_\gamma^{XX}(l) = \frac{1}{\sqrt{(2l+1)f_{\rm sky}}}\,\frac{\sigma_e^2}{2\bar{n}}, \qquad (26)$$

where $X = E, B$, $f_{\rm sky}$ is the fraction of sky covered by the survey, σ_e is the RMS intrinsic ellipticity of galaxies, and $\bar{n}$ is the number of source galaxies per steradian. In numbers, this yields

$$\frac{l(l+1)}{2\pi}\Delta C_\gamma^{XX}(l) \approx 1.6\times10^{-11}\left(\frac{l}{2}\right)^{3/2} f_{\rm sky}^{-1/2}\left(\frac{\sigma_e}{0.3}\right)^2 \times\left(\frac{\bar{n}}{100\,{\rm arcmin}^{-2}}\right)^{-1}. \qquad (27)$$

This prediction, for $f_{\rm sky} = 0.5$, is shown as black dotted line in Fig. 5. Clearly, one would need to go to source redshifts $\tilde{z} > 2$, at very high source densities, to detect a GW contribution at the level of $r = 0.2$ (unless the alignment strength at $z \sim 2$ is significantly larger than that measured at low redshifts).

Given the smallness of the signal and the possible contamination by scalar contributions (§ VI A), quantitative constraints on an inflationary GW background will thus be very challenging. Nevertheless, shear B-modes remain one of only a handful of probes in cosmology that can be used to search for such a background.

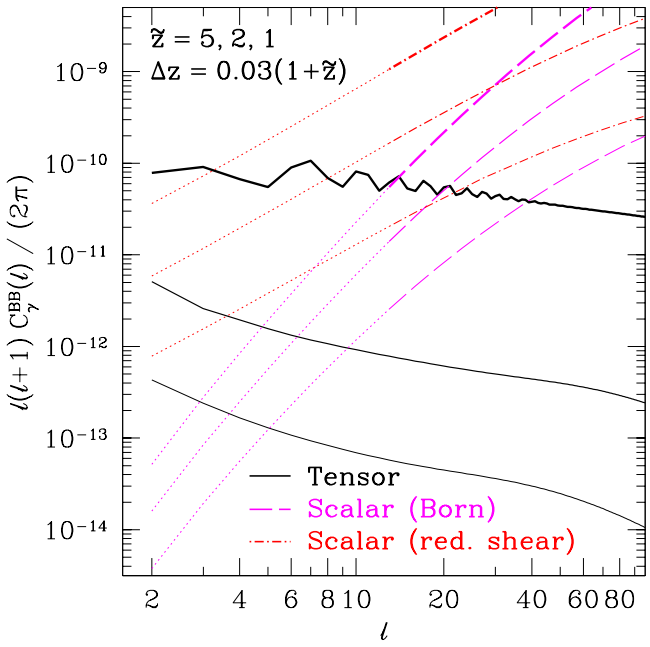

FIG. 7: Shear B-modes from tensor perturbations (black solid, including both lensing and intrinsic alignment) and second order scalar contributions from corrections to the Born approximation (magenta dashed) and reduced shear and lensing bias (assuming $q = 1$, red dash-dotted). Results are for redshifts $\tilde{z} = 5$, 2, 1 (from top to bottom). Note that the scalar contributions have been calculated using the Limber and flat-sky approximations, respectively, which are not accurate at $l \lesssim 10$ (dotted lines).

Acknowledgments

We would like to thank Jonathan Blazek, Chris Hirata, Marc Kamionkowski, Eiichiro Komatsu, Samuel Gralla, Uroš Seljak, and Masahiro Takada for helpful discussions. FS is supported by the Gordon and Betty Moore Foundation at Caltech. DJ was supported by NASA NNX12AE86G.

Appendix A: Fermi normal coordinates

In this appendix we review the basic concept of Fermi normal coordinates and its application to a flat FRW metric with perturbation h_{ij} of the spatial components (Eq. (1), but without imposing the transverse or tracefree conditions on h_{ij}). General covariance allows us to choose coordinates such that, at any given space-time point P, the metric is Minkowski and the Christoffel symbols vanish [29]; i.e.,

$$\begin{aligned} g_{\mu\nu} &= \eta_{\mu\nu} \\ g_{\mu\nu,\alpha} &= 0. \end{aligned} \tag{A1}$$

Riemann normal coordinates realize such coordinates by using a set of four geodesics (one time-like and three space-like) starting from the fixed point P. *Fermi* normal coordinates (FNC) are a specific extension of Riemann coordinates such that Eq. (A1) holds for every point along a fixed time-like geodesic. Specifically, we single out a time-like geodesic ("central geodesic") that passes through P, as the wordline of the observer around which the FNC are constructed. Given three space-like tangent vectors at P which are orthogonal to the tangent vector of the central geodesic at P, the tangent vectors at all other points along the central geodesic are defined through parallel transport. For all points along the central geodesic, we construct Riemann coordinates using these tangent vectors. Then, the condition Eq. (A1) is satisfied at all points along the central geodesic. Given a central geodesic, FNC are uniquely defined up to three Euler angles. The significance of FNC is that they are the natural coordinates in which an observer moving along the central geodesic would describe local experiments. With the conditions Eq. (A1) satisfied, the departure from Minkowski of the metric in FNC appears at quadratic order in the spatial Fermi coordinate x^i_F.

The Fermi normal coordinates can be explicitly constructed as follows (see [13, 30]). The time coordinate is chosen to coincide with the proper time along the central geodesic. Let $x^0_F(P) = t_P$ denote its value at point P. We can construct the spatial slicing of FNC, i.e. the $x^0_F = \text{const}$ hypersurface, as comprising all space-time points in the neighborhood of the central geodesic that are reached by a congruence of spatial geodesics whose tangent vector at P are orthogonal to the tangent vector of the central geodesic $(e_0)^\mu_P$. Let Q denote a point on this hypersurface, so that $x^0_F(Q) = t_P$. Further let $x^\mu(\lambda)$ be the unique geodesic (up to reparametrization) that connects P and Q. We can fix the affine parameter by requiring $x^\mu(0) = P,\ x^\mu(1) = Q$. We now expand $x^\mu(\lambda)$ in a power series in λ around $\lambda = 0$,

$$x^\mu(\lambda) = \sum_{n=0}^{\infty} \alpha^\mu_n \lambda^n. \tag{A2}$$

The requirement that $x^\mu(0) = P$ constrains α^μ_0 to be equal to the coordinates of P in the chosen, arbitrary coordinate system. Given a set of three orthonormal space-like unit vectors $(e_i)^\mu_P$ at P which are orthogonal to $(e_0)^\mu_P$, we can further write

$$\alpha^\mu_1 = \left.\frac{dx^\mu}{d\lambda}\right|_{\lambda=0} = x^i_F\,(e_i)^\mu_P\,. \tag{A3}$$

Since $(e_i)^\mu$ are parallel transported along the central geodesic, they are uniquely defined along the geodesic once they are specified at one point; i.e., they are unique up to three Euler angles. Eq. (A3) defines the spatial Fermi coordinate x^j_F (recall that we have defined λ through $x^\mu(\lambda = 1) = Q$, so that $\delta_{ij}x^i_F x^j_F$ provides a measure for the spatial distance between points Q and P).

In order to obtain the metric in the Fermi coordinate up to including $\mathcal{O}(x^2_F)$, we also need quadratic (α^μ_2) and cubic (α^μ_3) order coordinate transformation. For that, we use the geodesic equation:

$$\frac{d^2x^\mu}{d\lambda^2} + \Gamma^\mu_{\alpha\beta}\frac{dx^\alpha}{d\lambda}\frac{dx^\beta}{d\lambda} = 0. \tag{A4}$$

Rearranging the equation immediately yields

$$\begin{aligned} \left.\frac{d^2x^\mu}{d\lambda^2}\right|_{\lambda=0} = 2\alpha^\mu_2 = &-\Gamma^\mu_{\alpha\beta}\left.\frac{dx^\alpha}{d\lambda}\frac{dx^\beta}{d\lambda}\right|_{\lambda=0} = -\Gamma^\mu_{\alpha\beta}\Big|_P (e_i)^\alpha_P (e_j)^\beta_P x^i_F x^j_F \\ \alpha^\mu_2 = &-\frac{1}{2}\Gamma^\mu_{\alpha\beta}\Big|_P (e_i)^\alpha_P (e_j)^\beta_P x^i_F x^j_F. \end{aligned} \tag{A5}$$

Applying one more derivative with respect to λ to the geodesic equation yields α^μ_3 through

$$\begin{aligned} \alpha^\mu_3 &= \frac{1}{6}\left.\frac{d^3x^\mu}{d\lambda^3}\right|_{\lambda=0} = -\frac{1}{6}\frac{d}{d\lambda}\left(\Gamma^\mu_{\alpha\beta}\frac{dx^\alpha}{d\lambda}\frac{dx^\beta}{d\lambda}\right)\Bigg|_{\lambda=0} \\ &= -\frac{1}{6}\left[\Gamma^\mu_{\alpha\beta,\gamma} - 2\Gamma^\mu_{\sigma\alpha}\Gamma^\sigma_{\beta\gamma}\right]_P (e_i)^\alpha_P (e_j)^\beta_P (e_k)^\gamma_P x^i_F x^j_F x^k_F. \end{aligned} \tag{A6}$$

Combining all, we find the coordinate transformation from FNC to general coordinates on a fixed x_F^0 hypersurface, up to third order in x_F^i:

$$x^\mu(x_F^i)\Big|_{t_P} = x^\mu(P) + (e_i)^\mu_P\, x_F^i - \frac{1}{2}\Gamma^\mu_{\alpha\beta}\Big|_P (e_i)^\alpha_P (e_j)^\beta_P x_F^i x_F^j - \frac{1}{6}\left[\Gamma^\mu_{\alpha\beta,\gamma} - 2\Gamma^\mu_{\sigma\alpha}\Gamma^\sigma_{\beta\gamma}\right]_P (e_i)^\alpha_P (e_j)^\beta_P (e_k)^\gamma_P x_F^i x_F^j x_F^k. \quad \text{(A7)}$$

Here we have made explicit that $(e_\nu)^\mu$ and $\Gamma^\mu_{\alpha\beta}$ are always evaluated along the central geodesic at P. In App. A 1, we use this to derive the quadratic order FNC metric $g^F_{\mu\nu}$ for a given global metric $g_{\mu\nu}$ [Eq. (A23)]. This result is also given in Eq. (66) of [13] and Eq. (13.73) in [29]. In App. A 2 we then apply this procedure to the perturbed FRW metric in synchronous gauge [Eq. (1)] to obtain the Fermi coordinates and corrections $\propto x_F^2$ to the metric. Readers familiar with Fermi coordinates and Eq. (A23) may want to skip to App. A 2.

1. Metric in Fermi coordinate

In this section we derive the metric in the Fermi coordinate by using the coordinate transformation we have found in Eq. (A7). The final result will be that derived by [13], Eq. (A23). Under a coordinate transformation, the metric tensor transforms as

$$g^F_{\mu\nu}(x_F) = \frac{\partial x^\alpha}{\partial x_F^\mu}\frac{\partial x^\beta}{\partial x_F^\nu} g_{\alpha\beta}(x). \quad \text{(A8)}$$

Given the coordinate transform Eq. (A7), we derive the partial derivatives to second order in x_F, yielding

$$\begin{aligned}
\frac{\partial x^\mu}{\partial x_F^0} &= \frac{\partial x^\mu(P)}{\partial x_F^0} + \frac{\partial}{\partial x_F^0}(e_i)^\mu x_F^i - \frac{1}{2}\frac{\partial}{\partial x_F^0}\left[\Gamma^\mu_{\alpha\beta}\Big|_P (e_i)^\alpha (e_j)^\beta\right] x_F^i x_F^j \\
&= (e_0)^\mu - \Gamma^\mu_{\alpha\beta}\Big|_P (e_i)^\alpha (e_0)^\beta x_F^i - \frac{1}{2}\left[\Gamma^\mu_{\alpha\beta,\gamma} - 2\Gamma^\mu_{\sigma\beta}\Gamma^\sigma_{\gamma\alpha}\right]_P (e_0)^\gamma (e_i)^\alpha (e_j)^\beta x_F^i x_F^j \quad \text{(A9)} \\
\frac{\partial x^\mu}{\partial x_F^l} &= (e_l)^\mu - \Gamma^\mu_{\alpha\beta}\Big|_P (e_i)^\alpha (e_l)^\beta x_F^i - \frac{1}{6}\left[\Gamma^\mu_{\alpha\beta,\gamma} - 2\Gamma^\mu_{\sigma\gamma}\Gamma^\sigma_{\alpha\beta}\right]_P \left[(e_i)^\alpha (e_j)^\beta (e_l)^\gamma x_F^i x_F^j + 2(e_l)^\alpha (e_j)^\beta (e_k)^\gamma x_F^j x_F^k\right] \\
&= (e_l)^\mu - \Gamma^\mu_{\alpha\beta}\Big|_P (e_i)^\alpha (e_l)^\beta x_F^i - \frac{1}{6}\left[\Gamma^\mu_{\alpha\beta,\gamma} + 2\Gamma^\mu_{\gamma\alpha,\beta} - 2\Gamma^\mu_{\sigma\gamma}\Gamma^\sigma_{\alpha\beta} - 4\Gamma^\mu_{\sigma\beta}\Gamma^\sigma_{\gamma\alpha}\right]_P (e_i)^\alpha (e_j)^\beta (e_l)^\gamma x_F^i x_F^j, \quad \text{(A10)}
\end{aligned}$$

where all unit vectors are evaluated at P. Note that $\partial x^\mu(P)/\partial x_F^0 = (e_0)^\mu_P$, since by definition $(e_0)^\mu$ is the tangent vector to the central geodesic at P. Further, we have used that $(e_i)^\mu_P$ and $\Gamma^\mu_{\alpha\beta}\Big|_P$ only depend on x_F^0, and that by construction, the basis vectors $(e_i)^\mu$ are parallel transported along the central geodesic. This implies

$$\begin{aligned}
0 = \frac{D}{Dx_F^0}(e_i)^\alpha = (e_i)^\alpha_{;\mu}(e_0)^\mu &= \left[\frac{\partial}{\partial x^\mu}(e_i)^\alpha + \Gamma^\alpha_{\beta\mu}(e_i)^\beta\right](e_0)^\mu = \frac{\partial}{\partial x_F^0}(e_i)^\alpha + \Gamma^\alpha_{\beta\mu}(e_i)^\beta (e_0)^\mu \\
\Rightarrow \frac{\partial}{\partial x_F^0}(e_i)^\alpha &= -\Gamma^\alpha_{\beta\mu}(e_i)^\beta (e_0)^\mu. \quad \text{(A11)}
\end{aligned}$$

In Eq. (A9) we have also used

$$\frac{\partial}{\partial x_F^0}\Gamma^\mu_{\alpha\beta}\Big|_P = \Gamma^\mu_{\alpha\beta,\gamma}\Big|_P (e_0)^\gamma_P\,. \quad \text{(A12)}$$

Finally, we need to take into account that the metric on the right-hand side of Eq. (A8) is evaluated at a point Q (specified by x_F^i) away from the central geodesic. We perform a Taylor expansion of $g_{\mu\nu}$ around P,

$$g_{\alpha\beta}(Q) = g_{\alpha\beta}\Big|_P + g_{\alpha\beta,\mu}\Big|_P \delta x^\mu + \frac{1}{2} g_{\alpha\beta,\mu\nu}\Big|_P \delta x^\mu \delta x^\nu + \mathcal{O}(\delta x^3) \quad \text{(A13)}$$

where, from Eq. (A7),

$$\delta x^\mu = (e_i)^\mu_P\, x_F^i - \frac{1}{2}\Gamma^\mu_{\alpha_\beta}\,(e_i)^\alpha_P\,(e_j)^\beta_P\, x_F^i x_F^j \quad \text{(A14)}$$

That is, up to second order in x^i_F, the metric at Q is given by

$$g_{\alpha\beta}(Q) = g_{\alpha\beta}\Big|_P + g_{\alpha\beta,\mu}\Big|_P (e_i)^\mu_P x^i_F + \frac{1}{2}\left[g_{\alpha\beta,\mu\nu} - g_{\alpha\beta,\sigma}\Gamma^\sigma_{\mu\nu}\right]_P (e_i)^\mu_P (e_j)^\nu_P x^i_F x^j_F. \tag{A15}$$

From now on, every instance of $g_{\mu\nu}$, $\Gamma^\sigma_{\alpha\beta}$, and $(e_\nu)^\mu$ will be evaluated at P, and we will omit P for brevity hereafter. Inserting Eq. (A9), Eq. (A10) and Eq. (A15) into Eq. (A8), and expanding to second order in x^i_F yields the desired metric in FNC. At linear order, Eq. (A8) becomes

$$\begin{aligned} g^F_{\mu\nu} &= \left[(e_\mu)^\alpha - \Gamma^\alpha_{\rho\sigma}\,(e_i)^\rho\,(e_\mu)^\sigma\,x^i_F\right]\left[(e_\nu)^\beta - \Gamma^\beta_{\rho\sigma}\,(e_j)^\rho\,(e_\nu)^\sigma\,x^j_F\right]\left[g_{\alpha\beta} + g_{\alpha\beta,\kappa}(e_k)^\kappa x^k_F\right] \\ &= (e_\mu)^\alpha\,(e_\nu)^\beta\,g_{\alpha\beta} + \left(g_{\alpha\beta,\rho} - g_{\sigma\beta}\Gamma^\sigma_{\rho\alpha} - g_{\alpha\sigma}\Gamma^\sigma_{\rho\beta}\right)(e_\mu)^\alpha\,(e_\nu)^\beta\,(e_i)^\rho\,x^i_F \\ &= (e_\mu)^\alpha\,(e_\nu)^\beta\,g_{\alpha\beta} + g_{\alpha\beta;\rho}\,(e_\mu)^\alpha\,(e_\nu)^\beta\,(e_i)^\rho\,x^i_F = \eta_{\mu\nu}, \end{aligned} \tag{A16}$$

where the last equality follows from the definition of the orthonormal tetrad at P,

$$g_{\mu\nu}(e_\alpha)^\mu(e_\beta)^\nu = \eta_{\alpha\beta}, \tag{A17}$$

and the Levi-Civita connection, $g_{\mu\nu;\rho} = 0$.

Next, we calculate the quadratic correction to the metric in FNC,

$$\delta g^F_{00} = \left[\frac{1}{2}g_{\mu\nu,\alpha\beta} - \frac{1}{2}g_{\mu\nu,\sigma}\Gamma^\sigma_{\alpha\beta} - 2g_{\mu\gamma,\alpha}\Gamma^\gamma_{\beta\nu} - g_{\mu\gamma}\Gamma^\gamma_{\alpha\beta,\nu} + 2g_{\mu\gamma}\Gamma^\gamma_{\sigma\beta}\Gamma^\sigma_{\nu\alpha} + g_{\gamma\sigma}\Gamma^\gamma_{\alpha\mu}\Gamma^\sigma_{\beta\nu}\right](e_0)^\mu(e_0)^\nu(e_l)^\alpha(e_m)^\beta x^l_F x^m_F \tag{A18}$$

$$\begin{aligned} \delta g^F_{0i} = \Bigg[&\frac{1}{2}g_{\mu\nu,\alpha\beta} - \frac{1}{2}g_{\mu\nu,\sigma}\Gamma^\sigma_{\alpha\beta} - g_{\mu\gamma,\alpha}\Gamma^\gamma_{\beta\nu} - g_{\nu\gamma,\alpha}\Gamma^\gamma_{\beta\mu} - \frac{1}{2}g_{\nu\gamma}\Gamma^\gamma_{\alpha\beta,\mu} + g_{\nu\gamma}\Gamma^\gamma_{\sigma\alpha}\Gamma^\sigma_{\mu\beta} + g_{\gamma\sigma}\Gamma^\gamma_{\alpha\mu}\Gamma^\sigma_{\beta\nu} \\ &- \frac{1}{6}g_{\mu\lambda}\left(\Gamma^\lambda_{\alpha\beta,\nu} + 2\Gamma^\lambda_{\nu\alpha,\beta} - 2\Gamma^\lambda_{\sigma\nu}\Gamma^\sigma_{\alpha\beta} - 4\Gamma^\lambda_{\sigma\beta}\Gamma^\sigma_{\alpha\nu}\right)\Bigg](e_0)^\mu(e_i)^\nu(e_l)^\alpha(e_m)^\beta x^l_F x^m_F \end{aligned} \tag{A19}$$

$$\begin{aligned} \delta g^F_{ij} = \Bigg[&\frac{1}{2}g_{\mu\nu,\alpha\beta} - \frac{1}{2}g_{\mu\nu,\sigma}\Gamma^\sigma_{\alpha\beta} - 2g_{\mu\gamma,\alpha}\Gamma^\gamma_{\nu\beta} + g_{\gamma\sigma}\Gamma^\gamma_{\alpha\mu}\Gamma^\sigma_{\beta\nu} \\ &- \frac{1}{3}g_{\mu\lambda}\left(\Gamma^\lambda_{\alpha\beta,\nu} + 2\Gamma^\lambda_{\nu\alpha,\beta} - 2\Gamma^\lambda_{\sigma\nu}\Gamma^\sigma_{\alpha\beta} - 4\Gamma^\lambda_{\sigma\beta}\Gamma^\sigma_{\alpha\nu}\right)\Bigg](e_i)^\mu(e_j)^\nu(e_l)^\alpha(e_m)^\beta x^l_F x^m_F. \end{aligned} \tag{A20}$$

Finally, using

$$0 = g_{\mu\nu;\alpha} = g_{\mu\nu,\alpha} - g_{\sigma\nu}\Gamma^\sigma_{\mu\alpha} - g_{\mu\sigma}\Gamma^\sigma_{\nu\alpha}, \tag{A21}$$

we have

$$g_{\mu\nu,\alpha\beta} = g_{\mu\sigma}\Gamma^\sigma_{\nu\alpha,\beta} + g_{\sigma\nu}\Gamma^\sigma_{\mu\alpha,\beta} + g_{\mu\gamma}\Gamma^\gamma_{\sigma\beta}\Gamma^\sigma_{\nu\alpha} + g_{\gamma\nu}\Gamma^\gamma_{\sigma\beta}\Gamma^\sigma_{\mu\alpha} + g_{\gamma\sigma}\left(\Gamma^\gamma_{\mu\beta}\Gamma^\sigma_{\nu\alpha} + \Gamma^\gamma_{\nu\beta}\Gamma^\sigma_{\mu\alpha}\right). \tag{A22}$$

By using Eqs. (A21)–(A22), we write the partial derivatives of the metric as a function of the metric itself and the Christoffel symbols, to obtain the final expression for the FNC metric at quadratic order:

$$\begin{aligned} \delta g^F_{00} &= -R^F_{0l0m}x^l_F x^m_F \\ \delta g^F_{0i} &= -\frac{2}{3}R^F_{0lim}x^l_F x^m_F \\ \delta g^F_{ij} &= -\frac{1}{3}R^F_{iljm}x^l_F x^m_F. \end{aligned} \tag{A23}$$

Here, we have defined $R^F_{\alpha\beta\gamma\delta}$ as the Riemann tensor in FNC,

$$R^F_{\alpha\beta\gamma\delta} = (e_\alpha)^\mu(e_\beta)^\nu(e_\gamma)^\kappa(e_\delta)^\lambda\,R_{\mu\nu\kappa\lambda}, \tag{A24}$$

where the Riemann tensor is defined following the convention of [29]

$$R^\mu{}_{\alpha\beta\gamma} = \Gamma^\mu_{\alpha\gamma,\beta} - \Gamma^\mu_{\alpha\beta,\gamma} + \Gamma^\mu_{\sigma\beta}\Gamma^\sigma_{\alpha\gamma} - \Gamma^\mu_{\sigma\gamma}\Gamma^\sigma_{\alpha\beta}. \tag{A25}$$

2. Application to synchronous gauge metric

We write the perturbed FRW metric Eq. (1) in terms of proper time t instead of conformal time η,

$$ds^2 = -dt^2 + a^2(t)[\delta_{ij} + h_{ij}]dx^i dx^j. \tag{A26}$$

For this metric, coordinate time coincides with proper time for a comoving observer ($x^i = \text{const}$). Thus, without loss of generality we choose $\{(t,0,0,0)\}_t$ as central geodesic. Further, since the FNC time coordinate t_F is given by the proper time along the central geodesic, we have $t_F = t$ along the central geodesic (while $t_F \neq t$ away for $x^i_F \neq 0$). Correspondingly, the unit time vector is given by $(e_0)^\mu = (1,0,0,0)$, and orthogonal spatial basis vectors are given by (see also [31])

$$(e_k)^\mu = \left(0, \frac{1}{a}\left[\delta_{ik} - \frac{1}{2}h_{ik}\right]\right). \tag{A27}$$

The inverse metric is

$$g^{00} = -1,\ g^{ij} = \frac{1}{a^2}\left(\delta_{ij} - h_{ij}\right). \tag{A28}$$

This leads to the following Christoffel symbols,

$$\Gamma^0{}_{00} = \Gamma^0{}_{0i} = \Gamma^i_{00} = 0 \tag{A29}$$

$$\Gamma^0{}_{ij} = a^2 H\delta_{ij} + a^2 H h_{ij} + \frac{a^2}{2}\dot{h}_{ij} \tag{A30}$$

$$\Gamma^i{}_{0j} = H\delta_{ij} + \frac{1}{2}\dot{h}_{ij} \tag{A31}$$

$$\Gamma^i{}_{jk} = \frac{1}{2}\left(h_{ji,k} + h_{ki,j} - h_{jk,i}\right), \tag{A32}$$

where here and throughout, dots denote derivatives with respect to t. The Riemann tensor is given by

$$R^i{}_{00m} = \left(\dot{H} + H^2\right)\delta_{im} + \frac{1}{2}\ddot{h}_{im} + H\dot{h}_{im} \tag{A33}$$

$$R^n{}_{0im} = \frac{1}{2}\left(\dot{h}_{nm,i} - \dot{h}_{ni,m}\right) \tag{A34}$$

$$\begin{aligned} R^n{}_{ijm} &= a^2H^2\left[\delta_{nj}\delta_{im} - \delta_{nm}\delta_{ij}\right] + \frac{1}{2}\left(h_{mn,ij} + h_{ij,nm} - h_{im,nj} - h_{jn,im}\right) \\ &\quad + a^2H^2\left(h_{im}\delta_{nj} - h_{ij}\delta_{nm}\right) + \frac{a^2H}{2}\left(\dot{h}_{nj}\delta_{im} + \dot{h}_{im}\delta_{nj} - \dot{h}_{ij}\delta_{nm} - \dot{h}_{nm}\delta_{ij}\right). \end{aligned} \tag{A35}$$

We then have

$$R_{i00m} = g_{ij}R^j{}_{00m} = a^2\left(\dot{H} + H^2\right)\delta_{im} + a^2\left[\frac{1}{2}\ddot{h}_{im} + H\dot{h}_{im} + \left(\dot{H} + H^2\right)h_{im}\right] \tag{A36}$$

$$R_{l0im} = \frac{a^2}{2}\left(\dot{h}_{lm,i} - \dot{h}_{li,m}\right) \tag{A37}$$

$$\begin{aligned} R_{lijm} &= a^4H^2\left[\delta_{lj}\delta_{im} - \delta_{lm}\delta_{ij}\right] + \frac{a^2}{2}\left(h_{ml,ij} + h_{ij,lm} - h_{im,lj} - h_{jl,im}\right) \\ &\quad + a^4H^2\left(h_{im}\delta_{lj} + h_{lj}\delta_{im} - h_{ij}\delta_{lm} - h_{lm}\delta_{ij}\right) + \frac{a^4H}{2}\left(\dot{h}_{lj}\delta_{im} + \dot{h}_{im}\delta_{lj} - \dot{h}_{ij}\delta_{lm} - \dot{h}_{lm}\delta_{ij}\right). \end{aligned} \tag{A38}$$

Finally, the Riemann tensor in terms of FNC is given by

$$R^F_{l00m} = (e_l)^\mu (e_0)^\nu (e_0)^\kappa (e_m)^\lambda R_{\mu\nu\kappa\lambda} = \left(\dot{H} + H^2\right)\delta_{lm} + \left[\frac{1}{2}\ddot{h}_{lm} + H\dot{h}_{lm}\right] \tag{A39}$$

$$R^F_{l0im} = \frac{1}{2a}\left(\dot{h}_{lm,i} - \dot{h}_{li,m}\right) \tag{A40}$$

$$R^F_{lijm} = H^2\left[\delta_{lj}\delta_{im} - \delta_{lm}\delta_{ij}\right] + \frac{1}{2a^2}\left(h_{ml,ij} + h_{ij,lm} - h_{im,lj} - h_{jl,im}\right) + \frac{H}{2}\left(\dot{h}_{lj}\delta_{im} + \dot{h}_{im}\delta_{lj} - \dot{h}_{ij}\delta_{lm} - \dot{h}_{lm}\delta_{ij}\right). \tag{A41}$$

Combining all with Eq. (A23), we find that the metric in FNC is

$$
\begin{aligned}
g^F_{00} =& -1 + \left(\dot{H} + H^2\right) r_F^2 + \left[\frac{1}{2}\ddot{h}_{lm} + H\dot{h}_{lm}\right] x^l_F x^m_F. \\
g^F_{0i} =& \frac{1}{3}\left(\nabla_i \dot{h}_{lm} - \nabla_m \dot{h}_{li}\right) x^l_F x^m_F \\
g^F_{ij} =& \delta_{ij} + \frac{H^2}{3}\left[x^i_F x^j_F - r_F^2 \delta_{ij}\right] + \frac{1}{6}\left(\nabla_i\nabla_j h_{ml} + \nabla_l\nabla_m h_{ij} - \nabla_l\nabla_j h_{im} - \nabla_i\nabla_m h_{jl}\right) x^l_F x^m_F \\
&+ \frac{H}{6}\left(\dot{h}_{lj} x^l_F x^i_F + \dot{h}_{im} x^m_F x^j_F - \dot{h}_{ij} r_F^2 - \dot{h}_{lm} x^l_F x^m_F \delta_{ij}\right).
\end{aligned} \tag{A42}
$$

Here, we define $r_F^2 = \delta_{ij} x^i_F x^j_F$ and denote the partial derivative with respect to the FNC by $\nabla_i \equiv \partial/\partial x^i_F$. Note that in Eq. (A42), the derivative terms are already order x_F^2, hence we can use $\nabla_i = (1/a)\partial/\partial x^i$ here. We reiterate that Eq. (A42) is valid for any spatial metric perturbation h_{ij}, and thus also encompasses scalar cosmological perturbations written in synchronous-comoving gauge.

It is also useful to have an explicit expression for the transformation from global coordinates x^μ to Fermi coordinates x^ν_F. Evaluating Eq. (A7) for the metric Eq. (A26) yields

$$
x^i = \left(\delta_{ij} - \frac{1}{2}h_{ij}\right)\frac{1}{a}x^j_F - \frac{1}{2}\Gamma^i_{jk}\frac{1}{a^2}x^j_F x^k_F + \mathcal{O}(x_F^3) \tag{A43}
$$

$$
\frac{1}{a}x^i_F = \left(\delta_{ij} - \frac{1}{2}h_{ij}\right)x^j - \frac{1}{2}\Gamma^i_{jk}x^j x^k + \mathcal{O}(x^3). \tag{A44}
$$

This result is used in § VIIB of [1].

Finally, given the FNC metric Eq. (A42), we can derive the motion of non-relativistic bodies (of momentum p^i and mass m), which is governed by

$$
\frac{1}{m}\frac{dp^i}{dt} = \frac{1}{2}\, g^F_{00,i} = (H^2 + \dot{H})x^i_F - \nabla_i \Psi^F \tag{A45}
$$

$$
\Psi^F = -\frac{1}{2}\left(\frac{1}{2}\ddot{h}_{ij} + H\dot{h}_{ij}\right)x^i_F x^j_F. \tag{A46}
$$

This is the usual quasi-Newtonian equation of motion of a particle in an expanding Universe with peculiar potential Ψ^F. The effective potential induces a tidal tensor given by

$$
\begin{aligned}
t_{ij} \equiv& \left(\partial_i\partial_j - \frac{1}{3}\delta_{ij}\nabla^2\right)\Psi^F \\
=& -\frac{1}{2}\left(\frac{1}{2}\ddot{h}_{lm} + H\dot{h}_{lm}\right)\left(\partial_i\partial_j - \frac{1}{3}\delta_{ij}\nabla^2\right)x^l_F x^m_F \\
=& -\left[\left(\frac{1}{2}\ddot{h}_{lm} + H\dot{h}_{lm}\right) - \frac{1}{3}\delta_{ij}\mathrm{Tr}\left(\frac{1}{2}\ddot{h}_{lm} + H\dot{h}_{lm}\right)\right].
\end{aligned} \tag{A47}
$$

If h_{ij} is traceless, the last term vanishes and we obtain

$$
t_{ij} \overset{\text{traceless}}{=} -\left(\frac{1}{2}\ddot{h}_{lm} + H\dot{h}_{lm}\right). \tag{A48}
$$

Appendix B: Derivation of shear

1. Shear statistics from tensor modes

We express the tensor metric perturbation $h_{ij}(\tilde{\mathbf{x}}, \eta)$ as

$$
\begin{aligned}
h_{ij}(\tilde{\mathbf{x}}, \eta) =& \int \frac{d^3k}{(2\pi)^3}\left[e^+_{ij}(\hat{\mathbf{k}})h^+(\mathbf{k},\eta) + e^\times_{ij}(\hat{\mathbf{k}})h^\times(\mathbf{k},\eta)\right] e^{i\mathbf{k}\cdot\hat{\mathbf{n}}\,\tilde{\chi}} \\
=& \int \frac{d^3k}{(2\pi)^3}\sum_{p=-1,1} e^p_{ij}(\hat{\mathbf{k}})h_p(\mathbf{k},\eta)\, e^{i\mathbf{k}\cdot\hat{\mathbf{n}}\,\tilde{\chi}},
\end{aligned} \tag{B1}
$$

where we have defined the helicity± 2 polarization tensors and Fourier amplitudes through

$$\begin{aligned} e_{ij}^{\pm 1} &\equiv e_{ij}^{+} \pm i e_{ij}^{\times} \\ h_{\pm 1} &\equiv \frac{1}{2}(h_{+} \mp i h_{\times}). \end{aligned} \tag{B2}$$

In standard spherical coordinates, we have

$$m_{\pm}^{i} = \frac{1}{\sqrt{2}}\left(\hat{e}_{\theta} \mp i\hat{e}_{\phi}\right) = \frac{1}{\sqrt{2}} \begin{pmatrix} \cos\theta\cos\phi \pm i\sin\phi \\ \cos\theta\sin\phi \mp i\cos\phi \\ -\sin\theta \end{pmatrix}, \tag{B3}$$

where $\hat{e}_{\theta}$ and $\hat{e}_{\phi}$ are, respectively, the unit vectors of the polar and azimuthal angles. In order to make progress, we begin by evaluating the contribution of a single plane wave, assuming that $\mathbf{k} = k\hat{\mathbf{z}}$. We have

$$\begin{aligned} e_{\pm}^{p}(\hat{\mathbf{k}}, \hat{\mathbf{n}}) \equiv e_{ij}^{p}(\hat{\mathbf{k}}) m_{\mp}^{i}(\hat{\mathbf{n}}) m_{\mp}^{j}(\hat{\mathbf{n}}) &= \frac{1}{2}(1 \mp p\mu)^2 e^{i2p\phi} \\ e_{\parallel}^{p}(\hat{\mathbf{k}}) \equiv e_{ij}^{p}\hat{n}^{i}\hat{n}^{j} &= (1-\mu^2)e^{i2p\phi} \\ e_{ij}^{p}(\hat{\mathbf{k}}) m_{\mp}^{i}(\hat{\mathbf{n}})\hat{n}^{j} &= \frac{\sqrt{1-\mu^2}}{\sqrt{2}}(\mu \mp p)e^{i2p\phi}, \end{aligned} \tag{B4}$$

where $p = \pm 1$ and $\mu = \cos\theta$. We will also use the notation $k_{\pm} = m_{\mp}^{i} k_i = -\sin\theta\, k/\sqrt{2}$. Using Eq. (15) and Eq. (20), we then have for the contribution to the shear

$$\begin{aligned} ({}_{\pm 2}\gamma)(\mathbf{k}, \hat{\mathbf{n}}) = \sum_{p=-1,1} \Bigg\{ & -\frac{1}{2}\left[h_p(\mathbf{k}, \eta_0) + h_p(\mathbf{k}, \tilde{\eta}) e^{i\mathbf{k}\cdot\hat{\mathbf{n}}\,\tilde{\chi}}\right] e_{\pm}^{p} + \frac{1}{3} C_1 \rho_{\mathrm{cr}0} H_0^{-2} \tilde{a}^{-2} \left(h_p''(\mathbf{k}, \tilde{\eta}) + \tilde{a}\tilde{H} h_p'(\mathbf{k}, \tilde{\eta})\right) e^{i\mathbf{k}\cdot\hat{\mathbf{n}}, \tilde{\chi}} e_{\pm}^{p} \\ & - \int_0^{\tilde{\chi}} d\chi \left[\frac{\tilde{\chi} - \chi}{2}\frac{\chi}{\tilde{\chi}}(-k_{\pm}^2) e_{\parallel}^{p} + \left(1 - 2\frac{\chi}{\tilde{\chi}}\right) i k_{\pm} m_{\mp}^{k} \hat{n}^{l} e_{kl}^{p} - \frac{1}{\tilde{\chi}} e_{\pm}^{p}\right] h_p(\mathbf{k}, \eta_0 - \chi) e^{i\mathbf{k}\cdot\hat{\mathbf{n}}\,\chi} \Bigg\} \\ = \sum_{p=-1,1} \Bigg\{ & -\frac{1}{2}\left[h_p(\mathbf{k}, \eta_0) + \left(1 - \frac{2}{3} C_1 \rho_{\mathrm{cr}0} H_0^{-2} \tilde{a}^{-2} \left\{\partial_{\tilde{\eta}}^2 + \tilde{a}\tilde{H}\partial_{\tilde{\eta}}\right\}\right) h_p(\mathbf{k}, \tilde{\eta}) e^{i\mathbf{k}\cdot\hat{\mathbf{n}}\,\tilde{\chi}}\right] \frac{1}{2}(1 \mp p\mu)^2 e^{i2p\phi} \\ & + \int_0^{\tilde{\chi}} d\chi \left[\frac{\tilde{\chi} - \chi}{4}\frac{\chi}{\tilde{\chi}} k^2 (1-\mu^2)^2 + \left(1 - 2\frac{\chi}{\tilde{\chi}}\right) i\frac{k}{2}(1-\mu^2)(\mu \mp p) + \frac{1}{2\tilde{\chi}}(1 \mp p\mu)^2\right] \\ & \times e^{i2p\phi} h_p(\mathbf{k}, \eta_0 - \chi) e^{i\mathbf{k}\cdot\hat{\mathbf{n}}\,\chi} \Bigg\}. \end{aligned} \tag{B5}$$

Here, $\tilde{\eta} = \eta_0 - \tilde{\chi}$ is the conformal time at emission inferred from the observed redshift, and all tilded quantities are evaluated at the source redshift. The next step will be to derive the spherical harmonic coefficients of the shear. Clearly, all factors involve $e^{\pm i2\phi}$, so that only spherical harmonic coefficients with $m = \pm 2$ will be non-zero (this is of course a consequence of the choice $\mathbf{k} = k\hat{\mathbf{z}}$).

2. Spin-raising and lowering

Let us consider the case of ${}_2\gamma$, and restrict to one circular polarization $p = +1$ first:

$$\begin{aligned} {}_2\gamma(\mathbf{k}, \hat{\mathbf{n}}, +1) = & -\frac{1}{4}\left[h_1(\mathbf{k}, \eta_0) e^{ix\mu}\Big|_{x=0} + \left(1 - \frac{2}{3} C_1 \rho_{\mathrm{cr}0} H_0^{-2} \tilde{a}^{-2} \left\{\partial_{\tilde{\eta}}^2 + \tilde{a}\tilde{H}\partial_{\tilde{\eta}}\right\}\right) h_1(\mathbf{k}, \tilde{\eta}) e^{i\tilde{x}\mu}\right] (1-\mu)^2 e^{i2\phi} \\ & + \int_0^{\tilde{\chi}} d\chi \left[\frac{\tilde{\chi} - \chi}{4}\frac{\chi}{\tilde{\chi}} k^2 (1-\mu^2)^2 + \left(1 - 2\frac{\chi}{\tilde{\chi}}\right)\frac{ix}{2\chi}(1-\mu^2)(\mu - 1) + \frac{1}{2\tilde{\chi}}(1-\mu)^2\right] e^{i2\phi} h_1(\mathbf{k}, \eta_0 - \chi) e^{ix\mu}, \end{aligned} \tag{B6}$$

where we have defined $x = k\chi$, $\tilde{x} = k\tilde{\chi}$. Since this is a spin+2 quantity, we apply the spin-lowering operator twice to obtain a scalar. For this, we use that for functions that satisfy $\partial_\phi\, {}_s f = im\, {}_s f$ (see App. A of [1] and [32] for details),

$$\begin{aligned}\bar{\eth}^2\, {}_2f(\mu,\phi) &= \left(-\frac{\partial}{\partial\mu} + \frac{m}{1-\mu^2}\right)^2 \left[(1-\mu^2)\, {}_2f(\mu,\phi)\right] \\ \bar{\eth}^2\, {}_{-2}f(\mu,\phi) &= \left(-\frac{\partial}{\partial\mu} - \frac{m}{1-\mu^2}\right)^2 \left[(1-\mu^2)\, {}_{-2}f(\mu,\phi)\right]. \end{aligned} \tag{B7}$$

With $m = 2$, this yields

$$\begin{aligned}\bar{\eth}^2\, {}_2\gamma(\mathbf{k},\hat{\mathbf{n}},+1) =& -\frac{1}{4}\left(-\frac{\partial}{\partial\mu} + \frac{2}{1-\mu^2}\right)^2 \Bigg\{ \\ & (1-\mu^2)(1-\mu)^2 \left[h_1(\mathbf{k},\eta_0)e^{ix\mu}\Big|_{x=0} + \left(1 - \frac{2}{3}C_1\rho_{\rm cr0}H_0^{-2}\tilde{a}^{-2}\left\{\partial_{\tilde{\eta}}^2 + \tilde{a}\tilde{H}\partial_{\tilde{\eta}}\right\}\right) h_1(\mathbf{k},\tilde{\eta})e^{i\tilde{x}\mu}\right]\Bigg\} e^{i2\phi} \\ & + \int_0^{\tilde{\chi}} d\chi \left(-\frac{\partial}{\partial\mu} + \frac{2}{1-\mu^2}\right)^2 (1-\mu^2)\left[\frac{1}{4}\frac{\tilde{\chi}-\chi}{\chi\tilde{\chi}}x^2(1-\mu^2)^2 + \frac{1}{2}\frac{\tilde{\chi}-2\chi}{\chi\tilde{\chi}}ix(1-\mu^2)(\mu-1) + \frac{1}{2\tilde{\chi}}(1-\mu)^2\right] \\ & \qquad \times e^{i2\phi}h_1(\mathbf{k},\eta_0-\chi)e^{ix\mu} \\ =& -\frac{1}{4}\left(-\frac{\partial}{\partial\mu} + \frac{2}{1-\mu^2}\right)^2 \Bigg\{ \\ & (1-\mu^2)(1-\mu)^2 \left[h_1(\mathbf{k},\eta_0)e^{ix\mu}\Big|_{x=0} + \left(1 - \frac{2}{3}C_1\rho_{\rm cr0}H_0^{-2}\tilde{a}^{-2}\left\{\partial_{\tilde{\eta}}^2 + \tilde{a}\tilde{H}\partial_{\tilde{\eta}}\right\}\right) h_1(\mathbf{k},\tilde{\eta})e^{i\tilde{x}\mu}\right]\Bigg\} e^{i2\phi} \\ & + \int_0^{\tilde{\chi}} \frac{d\chi}{\chi}\left(-\frac{\partial}{\partial\mu} + \frac{2}{1-\mu^2}\right)^2 (1-\mu^2)\Bigg[\left(\frac{1}{4}x^2(1-\mu^2)^2 + \frac{1}{2}ix(1-\mu^2)(\mu-1)\right) \\ & \qquad + \frac{\chi}{\tilde{\chi}}\left(-\frac{1}{4}x^2(1-\mu^2)^2 - ix(1-\mu^2)(\mu-1) + \frac{1}{2}(1-\mu)^2\right)\Bigg] \\ & \qquad \times e^{i2\phi}h_1(\mathbf{k},\eta_0-\chi)e^{ix\mu} \\ =& \Bigg\{ -\frac{1}{4}\left[h_1(\mathbf{k},\eta_0)\left(\hat{Q}_1(x)e^{ix\mu}\right)\Big|_{x=0} + \left(1 - \frac{2}{3}C_1\rho_{\rm cr0}H_0^{-2}\tilde{a}^{-2}\left\{\partial_{\tilde{\eta}}^2 + \tilde{a}\tilde{H}\partial_{\tilde{\eta}}\right\}\right) h_1(\mathbf{k},\tilde{\eta})\hat{Q}_1(\tilde{x})e^{i\tilde{x}\mu}\right] \\ & + \int_0^{\tilde{\chi}} \frac{d\chi}{\chi}\left[\hat{Q}_2(x) + \frac{\chi}{\tilde{\chi}}\hat{Q}_3(x)\right]h_1(\mathbf{k},\eta_0-\chi)e^{ix\mu}\Bigg\}(1-\mu^2)e^{i2\phi}, \end{aligned} \tag{B8}$$

where we have turned powers of μ into powers of $-i\partial_x$ and defined derivative operators $\hat{Q}_i(x)$ as

$$\begin{aligned}\hat{Q}_1(x) &= 12 - x^2 + 8x\partial_x + x^2\partial_x^2 - i\left(8x + 2x^2\partial_x\right) \\ \hat{Q}_2(x) &= -\frac{1}{4}\left[14x^2 + x^4 + (40x + 14x^3)\partial_x + (50x^2 + 2x^4)\partial_x^2 + 14x^3\partial_x^3 + x^4\partial_x^4\right] - \frac{1}{2}i\left[4x + x^3 + 6x^2\partial_x + x^3\partial_x^2\right] \\ \hat{Q}_3(x) &= \frac{1}{4}\left[24 + 24x^2 + x^4 + (96x + 16x^3)\partial_x + (72x^2 + 2x^4)\partial_x^2 + 16x^3\partial_x^3 + x^4\partial_x^4\right]. \end{aligned} \tag{B9}$$

Although these operators are complicated, they will facilitate the connection with the convergence and rotation below. Note that, as expected, the real parts of $\hat{Q}_i(x)$ only involve even powers of x (counting derivatives as well), while the imaginary parts involve odd powers only (where $\mathrm{Im}\,\hat{Q}_3 = 0$). We now turn to $p = -1$:

$$\begin{aligned}{}_2\gamma(\mathbf{k},\hat{\mathbf{n}},-1) =& -\frac{1}{4}\left[h_{-1}(\mathbf{k},\eta_0)e^{ix\mu}\Big|_{x=0} + \left(1 - \frac{2}{3}C_1\rho_{\rm cr0}H_0^{-2}\tilde{a}^{-2}\left\{\partial_{\tilde{\eta}}^2 + \tilde{a}\tilde{H}\partial_{\tilde{\eta}}\right\}\right) h_{-1}(\mathbf{k},\tilde{\eta})e^{i\tilde{x}\mu}\right](1+\mu)^2 e^{-i2\phi} \\ & + \int_0^{\tilde{\chi}} d\chi\left[\frac{\tilde{\chi}-\chi}{4}\frac{\chi}{\tilde{\chi}}k^2(1-\mu^2)^2 + \left(1 - 2\frac{\chi}{\tilde{\chi}}\right)\frac{-ix}{2\chi}(1-\mu^2)(-\mu-1) + \frac{1}{2\tilde{\chi}}(1+\mu)^2\right]e^{-i2\phi}h_{-1}(\mathbf{k},\eta_0-\chi)e^{ix\mu}. \end{aligned} \tag{B10}$$

The appropriate spin-lowering operator is now for $m = -2$, i.e.

$$(-\partial_\mu - 2/(1-\mu^2))^2 = (\partial_\mu + 2/(1-\mu^2))^2 = (-\partial_{-\mu} + 2/(1-\mu^2))^2. \tag{B11}$$

Thus, ${}_2\gamma(\mathbf{k},\hat{\mathbf{n}},-1)$ is equal to ${}_2\gamma(\mathbf{k},\hat{\mathbf{n}},+1)$ [Eq. (B6)] when changing $\mu\to-\mu$, $x\to-x$ in addition to $h_1\to h_{-1}$, $\phi\to-\phi$. Since $\hat{Q}_i(-x)=\hat{Q}_i^*(x)$, we obtain

$$\bar{\eth}^2{}_2\gamma(\mathbf{k},\hat{\mathbf{n}},-1)=\Bigg\{-\frac{1}{4}\left[h_{-1}(\mathbf{k},\eta_0)\left(Q_1^*(x)e^{ix\mu}\right)\Big|_{x=0}+\left(1-\frac{2}{3}C_1\rho_{\rm cr0}H_0^{-2}\tilde{a}^{-2}\left\{\partial_{\tilde{\eta}}^2+\tilde{a}\tilde{H}\partial_{\tilde{\eta}}\right\}\right)h_{-1}(\mathbf{k},\tilde{\eta})Q_1^*(\tilde{x})e^{i\tilde{x}\mu}\right]$$
$$+\int_0^{\tilde{\chi}}\frac{d\chi}{\chi}\left[\hat{Q}_2^*(x)+\frac{\chi}{\tilde{\chi}}\hat{Q}_3^*(x)\right]e^{ix\mu}h_{-1}(\mathbf{k},\eta_0-\chi)\Bigg\}(1-\mu^2)e^{-i2\phi}. \tag{B12}$$

Similarly, we can derive the corresponding expressions for ${}_{-2}\gamma$,

$${}_{-2}\gamma(\mathbf{k},\hat{\mathbf{n}},+1)=-\frac{1}{4}\left[h_1(\mathbf{k},\eta_0)e^{ix\mu}\Big|_{x=0}+\left(1-\frac{2}{3}C_1\rho_{\rm cr0}H_0^{-2}\tilde{a}^{-2}\left\{\partial_{\tilde{\eta}}^2+\tilde{a}\tilde{H}\partial_{\tilde{\eta}}\right\}\right)h_1(\mathbf{k},\tilde{\eta})e^{i\tilde{x}\mu}\right](1+\mu)^2e^{i2\phi}$$
$$+\int_0^{\tilde{\chi}}d\chi\left[\frac{\tilde{\chi}-\chi}{4}\frac{\chi}{\tilde{\chi}}k^2(1-\mu^2)^2+\left(1-2\frac{\chi}{\tilde{\chi}}\right)\frac{-ix}{2\chi}(1-\mu^2)(-\mu-1)+\frac{1}{2\tilde{\chi}}(1+\mu)^2\right]e^{i2\phi}h_1(\mathbf{k},\eta_0-\chi)e^{ix\mu}, \tag{B13}$$

and correspondingly for $p=-1$, by acting twice with the spin-raising operator for $m=\pm2$, $(-\partial_\mu\mp2/(1-\mu^2))$. This immediately leads to

$$\eth^2{}_{-2}\gamma(\mathbf{k},\hat{\mathbf{n}},+1)=\Bigg\{-\frac{1}{4}\left[h_1(\mathbf{k},\eta_0)\left(Q_1^*(x)e^{ix\mu}\right)\Big|_{x=0}+\left(1-\frac{2}{3}C_1\rho_{\rm cr0}H_0^{-2}\tilde{a}^{-2}\left\{\partial_{\tilde{\eta}}^2+\tilde{a}\tilde{H}\partial_{\tilde{\eta}}\right\}\right)h_1(\mathbf{k},\tilde{\eta})Q_1^*(\tilde{x})e^{i\tilde{x}\mu}\right]$$
$$+\int_0^{\tilde{\chi}}\frac{d\chi}{\chi}\left[\hat{Q}_2^*(x)+\frac{\chi}{\tilde{\chi}}\hat{Q}_3^*(x)\right]e^{ix\mu}h_1(\mathbf{k},\eta_0-\chi)\Bigg\}(1-\mu^2)e^{i2\phi}$$
$$\eth^2{}_{-2}\gamma(\mathbf{k},\hat{\mathbf{n}},-1)=\Bigg\{-\frac{1}{4}\left[h_{-1}(\mathbf{k},\eta_0)\left(\hat{Q}_1(x)e^{ix\mu}\right)\Big|_{x=0}+\left(1-\frac{2}{3}C_1\rho_{\rm cr0}H_0^{-2}\tilde{a}^{-2}\left\{\partial_{\tilde{\eta}}^2+\tilde{a}\tilde{H}\partial_{\tilde{\eta}}\right\}\right)h_{-1}(\mathbf{k},\tilde{\eta})\hat{Q}_1(\tilde{x})e^{i\tilde{x}\mu}\right]$$
$$+\int_0^{\tilde{\chi}}\frac{d\chi}{\chi}\left[\hat{Q}_2(x)+\frac{\chi}{\tilde{\chi}}\hat{Q}_3(x)\right]e^{ix\mu}h_{-1}(\mathbf{k},\eta_0-\chi)\Bigg\}(1-\mu^2)e^{-i2\phi}. \tag{B14}$$

This is in the desired form of Eq. (A17) in App. A1 of [1], with azimuthal harmonic index $r=\pm2$. Since the shear ${}_{\pm2}\gamma$ is a spin±2 quantity, and $h_{\pm1}$ are two independent polarization states with power spectra $P_{h_{\pm1}}(k)=P_{T0}(k)/8$, we can apply Eq. (A24) in [1] with $s=2$, $r=2$, $N_P=2$, and $P_h=P_{T0}/8$:

$$C_\gamma^{XX}(l)=\frac{1}{2\pi}\int k^2dk\,P_{T0}(k)|F_l^{\gamma X}(k)|^2 \tag{B15}$$
$$F_l^{\gamma E}(k)\equiv-\frac{1}{4}\left[T_T(k,\eta_0)\left(\mathrm{Re}\,\hat{Q}_1(x)\frac{j_l(x)}{x^2}\right)_{x=0}+\left(1-\frac{2}{3}C_1\rho_{\rm cr0}H_0^{-2}\tilde{a}^{-2}\left\{\partial_{\tilde{\eta}}^2+\tilde{a}\tilde{H}\partial_{\tilde{\eta}}\right\}\right)T_T(k,\tilde{\eta})\mathrm{Re}\,\hat{Q}_1(\tilde{x})\frac{j_l(\tilde{x})}{\tilde{x}^2}\right]$$
$$+\int_0^{\tilde{\chi}}\frac{d\chi}{\chi}\left[\mathrm{Re}\,\hat{Q}_2(x)+\frac{\chi}{\tilde{\chi}}\mathrm{Re}\,\hat{Q}_3(x)\right]\frac{j_l(x)}{x^2}T_T(k,\eta_0-\chi)$$
$$F_l^{\gamma B}(k)\equiv-\frac{1}{4}\left[T_T(k,\eta_0)\left(\mathrm{Im}\,\hat{Q}_1(x)\frac{j_l(x)}{x^2}\right)_{x=0}+\left(1-\frac{2}{3}C_1\rho_{\rm cr0}H_0^{-2}\tilde{a}^{-2}\left\{\partial_{\tilde{\eta}}^2+\tilde{a}\tilde{H}\partial_{\tilde{\eta}}\right\}\right)T_T(k,\tilde{\eta})\mathrm{Im}\,\hat{Q}_1(\tilde{x})\frac{j_l(\tilde{x})}{\tilde{x}^2}\right]$$
$$+\int_0^{\tilde{\chi}}\frac{d\chi}{\chi}\left[\mathrm{Im}\,\hat{Q}_2(x)+\frac{\chi}{\tilde{\chi}}\mathrm{Im}\,\hat{Q}_3(x)\right]\frac{j_l(x)}{x^2}T_T(k,\eta_0-\chi).$$

Again, $\tilde{\eta} = \eta_0 - \tilde{\chi}$, $\tilde{a} = a(\tilde{\eta})$, and $x = k\chi$, $\tilde{x} = k\tilde{\chi}$. This completes the derivation of the angular power spectrum of E- and B-modes of the shear. The operators $\hat{Q}_i$ when applied to spherical Bessel functions can be simplified to yield

$$\begin{aligned}
\mathrm{Re}\,\hat{Q}_1(x)\frac{j_l(x)}{x^2} &= -\frac{1}{x^2}\left[(2x^2 - l^2 - 3l - 2)j_l(x) + 2xj_{l+1}(x)\right] \\
\mathrm{Im}\,\hat{Q}_1(x)\frac{j_l(x)}{x^2} &= -\frac{1}{x}\left[2(l+2)j_l(x) - 2xj_{l+1}(x)\right] \\
&= 2\left[(l-1)\frac{j_l(x)}{x} - j_{l-1}(x)\right] \\
\mathrm{Re}\,\hat{Q}_2(x)\frac{j_l(x)}{x^2} &= -\frac{1}{4}\left[(l^4 - 5l^2 + 4)\frac{j_l(x)}{x^2} + 2(l^2 + l - 2)\frac{j_{l+1}(x)}{x}\right] \\
&= -\frac{1}{4}(l+2)(l-1)\left[(l+1)(l-2)\frac{j_l(x)}{x^2} + 2\frac{j_{l+1}(x)}{x}\right] \\
\mathrm{Im}\,\hat{Q}_2(x)\frac{j_l(x)}{x^2} &= -\frac{(l-1)(l+2)}{2}\frac{j_l(x)}{x} \\
\mathrm{Re}\,\hat{Q}_3(x)\frac{j_l(x)}{x^2} &= \frac{1}{4}\frac{(l+2)!}{(l-2)!}\frac{j_l(x)}{x^2} \\
\mathrm{Im}\,\hat{Q}_3(x)\frac{j_l(x)}{x^2} &= 0.
\end{aligned} \tag{B16}$$

In the limit of $x \to 0$ for $l = 2$, we have

$$\begin{aligned}
\mathrm{Re}\,\hat{Q}_1(x)\frac{j_2(x)}{x^2} &\overset{x\to 0}{=} \frac{4}{5} \\
\mathrm{Re}\,\hat{Q}_3(x)\frac{j_2(x)}{x^2} &\overset{x\to 0}{=} \frac{2}{5},
\end{aligned} \tag{B17}$$

while all other operators vanish in this limit for $l = 2$, and all operators vanish in this limit for $l > 2$. With this, we can easily verify that modes with $k \to 0$ do not contribute to the quadrupole, as desired. As we let $k \to 0$, and thus $x \to 0$, we trivially have $F_l^{\gamma B}(k) \to 0$, and

$$F_l^{\gamma E}(k) \overset{k\to 0}{=} -\frac{1}{4}2\left(\frac{4}{5}\right) + \int_0^{\tilde{\chi}} \frac{d\chi}{\chi}\frac{\chi}{\tilde{\chi}}\left(\frac{2}{5}\right) = -\frac{2}{5} + \frac{2}{5} = 0, \tag{B18}$$

where we have used that $T_T(k \to 0, \eta) \to 1$ (of course, we only need the fact that $T_T(k \to 0, \eta) \to$ const).

Appendix C: Connection to convergence and rotation

In this section, we cross-check Eq. (B15) with the angular power spectra of coordinate convergence and rotation, through the relations Eq. (23).

1. Angular power spectrum of coordinate convergence

We begin with the general expression for the coordinate convergence $\hat{\kappa} \equiv -1/2\partial_{\perp i}\Delta x^i_\perp$ derived in [1], restricted to synchronous-comoving gauge, and assuming a tranverse-traceless metric perturbation h_{ij}:

$$\begin{aligned}
\hat{\kappa} &= \frac{3}{4}(h_\parallel)_o + \frac{1}{2}\int_0^{\tilde{\chi}} d\chi\left[-\partial_\parallel h_\parallel - \frac{3}{\chi}h_\parallel + (\tilde{\chi} - \chi)\frac{\chi}{\tilde{\chi}}\nabla_\perp^2\left\{-\frac{1}{2}h_\parallel\right\}\right] \\
&= \frac{3}{4}(h_\parallel)_o + \int_0^{\tilde{\chi}} d\chi\left[-\frac{1}{2}\partial_\parallel h_\parallel - \frac{3}{2\chi}h_\parallel\right] - \frac{1}{4}\nabla_\Omega^2\int_0^{\tilde{\chi}} d\chi\frac{\tilde{\chi} - \chi}{\chi\tilde{\chi}}h_\parallel.
\end{aligned} \tag{C1}$$

This is equivalent to the expression used in [7], but in a form more convenient for the comparison with the shear. Considering a single plane-wave perturbation oriented along the z-axis, with $+1$ circular polarization, we have

$$\hat{\kappa}(\hat{\mathbf{n}},\mathbf{k},+1) = \frac{3}{4}(1-\mu^2)e^{i2\phi}e^{ix\mu}\Big|_{x=0} h_1(\mathbf{k},\eta_0) + \int_0^{\tilde{\chi}} d\chi \left[-\frac{1}{2\chi}x\partial_x - \frac{3}{2\chi}\right](1-\mu^2)e^{i2\phi}e^{ix\mu}h_1(\mathbf{k},\eta) - \frac{1}{4}\nabla^2_\Omega \int_0^{\tilde{\chi}} d\chi \frac{\tilde{\chi}-\chi}{\chi\tilde{\chi}}(1-\mu^2)e^{i2\phi}e^{ix\mu}h_1(\mathbf{k},\eta), \tag{C2}$$

where we have used Eq. (B4), and turned $i\mu k$ into $x/\chi\partial_x$, understanding that the derivative only acts on $e^{ix\mu}$. In order to derive the multipole moments of $\hat{\kappa}$, we now use the relation (see App. A in [1])

$$\int d\Omega\, Y^*_{lm}(1-\mu^2)e^{\pm i2\phi}e^{ix\mu} = -\sqrt{4\pi(2l+1)}\sqrt{\frac{(l+2)!}{(l-2)!}}\, i^l \frac{j_l(x)}{x^2}\delta_{m\pm2}, \tag{C3}$$

which yields

$$a^{\hat{\kappa}}_{lm}(\mathbf{k}) = -\sqrt{\frac{2l+1}{4\pi}\frac{(l+2)!}{(l-2)!}}(4\pi)i^l\delta_{m2}\left[\frac{3}{4}h_1(\mathbf{k},\eta_0)\frac{j_l(x)}{x^2}\Big|_{x=0} + \int d\chi\, h_1(\mathbf{k},\eta)\left\{-\frac{1}{2\chi}x\partial_x - \frac{3}{2\chi} + \frac{1}{4}l(l+1)\frac{\tilde{\chi}-\chi}{\chi\tilde{\chi}}\right\}\frac{j_l(x)}{x^2}\right]. \tag{C4}$$

We thus obtain for the angular power spectrum of $\hat{\kappa}$:

$$\begin{aligned} C_{\hat{\kappa}}(l) &= \frac{1}{2\pi}\int k^2 dk\, P_{T0}(k)|F^{\hat{\kappa}}_l(k)|^2 \\ F^{\hat{\kappa}}_l(k) &= \sqrt{\frac{(l+2)!}{(l-2)!}}\left[-\frac{3}{4}T_T(k,\eta_0)\frac{j_l(x)}{x^2}\Big|_{x=0} - \int\frac{d\chi}{\chi}\,T_T(k,\eta_0-\chi)\left\{-\frac{1}{2}x\partial_x - \frac{3}{2} + \frac{1}{4}l(l+1)\left(1-\frac{\chi}{\tilde{\chi}}\right)\right\}\frac{j_l(x)}{x^2}\right] \\ &= \sqrt{\frac{l(l+1)}{(l+2)(l-1)}}\left[-(l+2)(l-1)\frac{3}{4}T_T(k,\eta_0)\frac{1}{15}\delta_{l2}\right. \\ &\qquad \left. -(l+2)(l-1)\int\frac{d\chi}{\chi}\,T_T(k,\eta_0-\chi)\left\{-\frac{1}{2}x\partial_x - \frac{3}{2} + \frac{1}{4}l(l+1)\left(1-\frac{\chi}{\tilde{\chi}}\right)\right\}\frac{j_l(x)}{x^2}\right], \end{aligned} \tag{C5}$$

where for the observer term we have used $\lim_{x\to0} j_l(x)/x^2 = 1/15$ for $l=2$, and 0 for $l>2$. We can now simplify the operator applied to the spherical Bessel function, using the recurrence relation $j_l' = l/x\, j_l - j_{l+1}$, yielding

$$\begin{aligned} \left\{-\frac{1}{2}x\partial_x - \frac{3}{2} + \frac{1}{4}l(l+1)\right\}\frac{j_l(x)}{x^2} &= -\frac{1}{2}\left\{[l+1-\frac{1}{2}l(l+1)]\frac{j_l}{x^2} - \frac{j_{l+1}}{x}\right\} \\ &= \frac{1}{4}(l-2)(l+1)\frac{j_l}{x^2} + \frac{1}{2}\frac{j_{l+1}}{x}. \end{aligned} \tag{C6}$$

We thus have

$$F^{\hat{\kappa}}_l(k) = \sqrt{\frac{l(l+1)}{(l+2)(l-1)}}\left[-\frac{1}{5}T_T(k,\eta_0)\delta_{l2} - \int\frac{d\chi}{\chi}\,T_T(k,\eta_0-\chi)\left[\frac{(l+2)(l-1)}{4}\left\{(l-2)(l+1)\frac{j_l}{x^2} + 2\frac{j_{l+1}}{x}\right\} - \frac{1}{4}\frac{\chi}{\tilde{\chi}}\frac{(l+2)!}{(l-2)!}\frac{j_l(x)}{x^2}\right]\right]. \tag{C7}$$

For comparison, the corresponding filter function for the E-mode of the shear is (without metric shear and IA contributions, as discussed in § V A)

$$F^{\gamma E}_l(k) = -\frac{1}{5}T_T(k,\eta_0)\delta_{l2} - \int_0^{\tilde{\chi}}\frac{d\chi}{\chi}\left[\frac{(l+2)(l-1)}{4}\left\{(l+1)(l-2)\frac{j_l(x)}{x^2} + 2\frac{j_{l+1}(x)}{x}\right\} - \frac{\chi}{\tilde{\chi}}\frac{1}{4}\frac{(l+2)!}{(l-2)!}\frac{j_l(x)}{x^2}\right]T_T(k,\eta_0-\chi), \tag{C8}$$

where we have used the $x \to 0$ limit for $\mathrm{Re}\,\hat{Q}_1 j_l/x^2$ for the observer term. Hence,

$$F_l^{\gamma E}(k) = \sqrt{\frac{(l+2)(l-1)}{l(l+1)}} F_l^{\hat{\kappa}}(k). \tag{C9}$$

Our result for the shear (without metric shear and intrinsic alignment) thus recovers the full-sky relation between shear E-(gradient-)modes and coordinate convergence Eq. (23).

2. Angular power spectrum of rotation

Using the definition of the rotation Eq. (22), and the expression for $\Delta x^i_\perp$ [Eq. (36) in [1]] restricted to synchronous gauge, we obtain

$$\begin{aligned}\omega &= \frac{1}{2}\int_0^{\tilde{\chi}} d\chi \Big[\varepsilon_{ijk}\hat{n}^i(\partial^j_\perp h^k_{\ m})\hat{n}^m\Big] \\ &= \frac{1}{2}\int_0^{\tilde{\chi}} d\chi \Big[\varepsilon_{ijk}h^k_{\ m}{}^{,j}\Big]\hat{n}^i\hat{n}^m.\end{aligned} \tag{C10}$$

Note that $\varepsilon_{ijk}\partial^j_\perp \hat{n}^k = \varepsilon_{ijk}\partial^j \hat{n}^k = 0$, and $\hat{n}^j \partial_{\perp j} f(\mathbf{x},\eta) = 0$, and that pulling the derivatives inside the integrand yields a factor of $\chi/\tilde{\chi}$. This result agrees with Eq. (4) in [8] (this ω is also equivalent to $\nabla^2_\theta\Omega$ as defined above Eq. (19) of [6]). We now calculate the angular power spectrum of ω. Assuming as above a single plane wave with $\mathbf{k} = k\hat{\mathbf{z}}$, we have

$$\begin{aligned}\varepsilon_{ijk}h^k_{\ m}{}^{,j}\hat{n}^i\hat{n}^m &= -ik\left[-2\hat{n}^1\hat{n}^2 h_+ + \left((\hat{n}^1)^2 - (\hat{n}^2)^2\right)h_\times\right]e^{i\mathbf{k}\cdot\mathbf{x}} \\ &= -ik(1-\mu^2)\left[-\sin 2\phi h_+ + \cos 2\phi h_\times\right]e^{ik\chi\mu} \\ &= k(1-\mu^2)\left[h_1 e^{2i\phi} - h_{-1}e^{-2i\phi}\right]e^{ik\chi\mu},\end{aligned} \tag{C11}$$

since $h_{-1} = h_1^*$. Thus,

$$\omega(\hat{\mathbf{n}},\mathbf{k}) = \frac{1}{2}\int_0^{\tilde{\chi}} d\chi\, k\left[h_1 e^{2i\phi} - h_{-1}e^{-2i\phi}\right](1-\mu^2)e^{ik\chi\mu}. \tag{C12}$$

Note the relative minus sign between the two polarization states which shows that ω is parity-odd. In analogy with the derivation for $\hat{\kappa}$ (see also App. A1 in [1]) we use Eq. (C3) to obtain the angular power spectrum of the rotation (it only contains "B-modes"):

$$C_\omega^{BB}(l) = \frac{1}{2\pi}\int k^2 dk\, P_{T0}(k)|F_l^\omega(k)|^2 \tag{C13}$$

$$F_l^\omega(k) \equiv -\frac{1}{2}\sqrt{\frac{(l+2)!}{(l-2)!}}\int \frac{d\chi}{\chi}\, x\, T_T(k,\eta_0-\chi)\frac{j_l(x)}{x^2}\Big|_{x=k\chi}. \tag{C14}$$

In Dodelson et al. [8], an additional "metric shear" term was added to $F_l^\omega(k)$:

$$\begin{aligned}F_l^\omega &\to F_l^\omega + F_l^{\omega\,\mathrm{MS}} \\ F_l^{\omega\,\mathrm{MS}}(k) &= -\frac{1}{2}\frac{1}{(l+2)(l-1)}\sqrt{\frac{(l+2)!}{(l-2)!}}\left[(l-1)\frac{j_l(\tilde{x})}{\tilde{x}} - j_{l-1}(\tilde{x})\right]T_T(k,\tilde{\eta}).\end{aligned} \tag{C15}$$

Note that in our convention, there is an overall minus sign for both F_l^ω and $F_l^{\omega,\mathrm{MS}}$. Next, consider the B-mode power spectrum of the shear without observer, IA and FNC terms, Eq. (B15) with

$$\begin{aligned}F_l^{\gamma B}(k) &= -\frac{1}{2}(l+2)(l-1)\int_0^{\tilde{\chi}}\frac{d\chi}{\chi}x\,T_T(k,\eta_0-\chi)\frac{j_l(x)}{x^2} \\ &= \sqrt{\frac{(l+2)(l-1)}{l(l+1)}}F_l^\omega(k),\end{aligned} \tag{C16}$$

where we have used Eq. (B16) and Eq. (C14). We thus recover the relation Eq. (23) between the B-modes of the shear and the rotation (without "metric shear"). The contribution of the FNC term to the B-modes of the shear is given by

$$F_l^{\gamma B\,\mathrm{FNC}}(k) = -\frac{1}{4}T_T(k,\tilde{\eta})\mathrm{Im}\,\hat{Q}_1(\tilde{x})\frac{j_l(\tilde{x})}{\tilde{x}^2} = -\frac{1}{2}T_T(k,\tilde{\eta})\left[(l-1)\frac{j_l(\tilde{x})}{\tilde{x}} - j_{l-1}(\tilde{x})\right]$$
$$= \sqrt{\frac{(l+2)(l-1)}{l(l+1)}}F_l^{\omega\,\mathrm{MS}}(k), \tag{C17}$$

showing that the "metric shear" contribution to ω derived in [8] agrees with the contribution of the FNC term to the shear B-modes.

[1] F. Schmidt and D. Jeong (2012), 1204.3625.
[2] U. Seljak and M. Zaldarriaga, Physical Review Letters **78**, 2054 (1997), arXiv:astro-ph/9609169.
[3] M. Kamionkowski, A. Kosowsky, and A. Stebbins, Phys. Rev. Lett. **78**, 2058 (1997), URL `http://link.aps.org/doi/10.1103/PhysRevLett.78.2058`.
[4] A. Cooray, New Astronomy **9**, 173 (2004), arXiv:astro-ph/0309301.
[5] K. W. Masui and U.-L. Pen, Physical Review Letters **105**, 161302 (2010), 1006.4181.
[6] L. G. Book, M. Kamionkowski, and T. Souradeep, ArXiv e-prints (2011), 1109.2910.
[7] D. Jeong and F. Schmidt (2012), 1205.1512.
[8] S. Dodelson, E. Rozo, and A. Stebbins, Physical Review Letters **91**, 021301 (2003), arXiv:astro-ph/0301177.
[9] L. Book, M. Kamionkowski, and F. Schmidt, ArXiv e-prints (2011), 1112.0567.
[10] D. Sarkar, P. Serra, A. Cooray, K. Ichiki, and D. Baumann, Phys. Rev. D **77**, 103515 (2008), 0803.1490.
[11] S. Dodelson, Phys. Rev. D **82**, 023522 (2010), 1001.5012.
[12] E. Fermi, Atti Acad. Naz. Lincei Rend. Cl. Sci. Fiz. Mat. Nat. **31**, 21 (1922).
[13] F. K. Manasse and C. W. Misner, Journal of Mathematical Physics **4**, 735 (1963).
[14] N. Kaiser and A. Jaffe, Astrophys. J. **484**, 545 (1997), arXiv:astro-ph/9609043.
[15] E. Komatsu, K. M. Smith, J. Dunkley, C. L. Bennett, B. Gold, G. Hinshaw, N. Jarosik, D. Larson, M. R. Nolta, L. Page, et al., Astrophys. J. Supp. **192**, 18 (2011), 1001.4538.
[16] P. Catelan, M. Kamionkowski, and R. D. Blandford, MNRAS **320**, L7 (2001), arXiv:astro-ph/0005470.
[17] C. M. Hirata and U. Seljak, Phys. Rev. D **70**, 063526 (2004), arXiv:astro-ph/0406275.
[18] M. L. Brown, A. N. Taylor, N. C. Hambly, and S. Dye, MNRAS **333**, 501 (2002), arXiv:astro-ph/0009499.
[19] J. Blazek, M. McQuinn, and U. Seljak, JCAP **5**, 10 (2011), 1101.4017.
[20] B. Joachimi, R. Mandelbaum, F. B. Abdalla, and S. L. Bridle, Astron. Astrophys. **527**, A26 (2011), 1008.3491.
[21] A. Stebbins, ArXiv Astrophysics e-prints (1996), arXiv:astro-ph/9609149.
[22] S. Mollerach, D. Harari, and S. Matarrese, Phys. Rev. D **69**, 063002 (2004), arXiv:astro-ph/0310711.
[23] D. Baumann, P. Steinhardt, K. Takahashi, and K. Ichiki, Phys. Rev. D **76**, 084019 (2007), arXiv:hep-th/0703290.
[24] C. M. Hirata and U. Seljak, Phys. Rev. D **68**, 083002 (2003), arXiv:astro-ph/0306354.
[25] A. Cooray and W. Hu, Astrophys. J. **574**, 19 (2002), astro-ph/0202411.
[26] P. Schneider, L. van Waerbeke, B. Jain, and G. Kruse (1997), astro-ph/9708143.
[27] S. Dodelson, C. Shapiro, and M. J. White, Phys. Rev. **D73**, 023009 (2006), astro-ph/0508296.
[28] F. Schmidt, E. Rozo, S. Dodelson, L. Hui, and E. Sheldon, Astrophys. J. **702**, 593 (2009), 0904.4703.
[29] C. W. Misner, K. S. Thorne, and J. A. Wheeler, *Gravitation* (1973).
[30] T. Baldauf, U. Seljak, L. Senatore, and M. Zaldarriaga, ArXiv e-prints (2011), 1106.5507.
[31] D. Jeong, F. Schmidt, and C. M. Hirata, Phys. Rev. D **85**, 023504 (2012), 1107.5427.
[32] M. Zaldarriaga and U. Seljak, Phys. Rev. D **55**, 1830 (1997), URL `http://link.aps.org/doi/10.1103/PhysRevD.55.1830`.